



**NAVAL  
POSTGRADUATE  
SCHOOL**

**MONTEREY, CALIFORNIA**

**THESIS**

**THE INFLUENCE OF WIND ON  
HF RADAR SURFACE CURRENT FORECASTS**

by

Francisco Moisés Soares Calisto de Almeida

December 2008

Thesis Advisor:  
Second Reader:

Jeffrey Paduan  
Curtis Collins

**Approved for public release; distribution is unlimited**

THIS PAGE INTENTIONALLY LEFT BLANK

<b>REPORT DOCUMENTATION PAGE</b>			<i>Form Approved OMB No. 0704-0188</i>
Public reporting burden for this collection of information is estimated to average 1 hour per response, including the time for reviewing instruction, searching existing data sources, gathering and maintaining the data needed, and completing and reviewing the collection of information. Send comments regarding this burden estimate or any other aspect of this collection of information, including suggestions for reducing this burden, to Washington headquarters Services, Directorate for Information Operations and Reports, 1215 Jefferson Davis Highway, Suite 1204, Arlington, VA 22202-4302, and to the Office of Management and Budget, Paperwork Reduction Project (0704-0188) Washington DC 20503.			
<b>1. AGENCY USE ONLY (Leave blank)</b>	<b>2. REPORT DATE</b> December 2008	<b>3. REPORT TYPE AND DATES COVERED</b> Master's Thesis	
<b>4. TITLE AND SUBTITLE</b> The Influence of Wind on HF Surface Current Forecasts		<b>5. FUNDING NUMBERS</b>	
<b>6. AUTHOR(S)</b> Francisco M. S. C. de Almeida		<b>8. PERFORMING ORGANIZATION REPORT NUMBER</b>	
<b>7. PERFORMING ORGANIZATION NAME(S) AND ADDRESS(ES)</b> Naval Postgraduate School Monterey, CA 93943-5000		<b>10. SPONSORING/MONITORING AGENCY REPORT NUMBER</b>	
<b>9. SPONSORING /MONITORING AGENCY NAME(S) AND ADDRESS(ES)</b> N/A		<b>11. SUPPLEMENTARY NOTES</b> The views expressed in this thesis are those of the author and do not reflect the official policy or position of the Department of Defense or the U.S. Government.	
<b>12a. DISTRIBUTION / AVAILABILITY STATEMENT</b> Approved for public release; distribution is unlimited.		<b>12b. DISTRIBUTION CODE</b>	
<b>13. ABSTRACT (maximum 200 words)</b> <p>The ability to predict surface currents can have a beneficial impact in several activities such as Search and Rescue and Oil Spill Response, as well as others more purely scientific, operational or economic. The Naval Postgraduate School, in conjunction with the Romberg Tiburon Center and the University of California Santa Barbara, has been studying this purpose for the Coastal Response Research Center, University of New Hampshire and NOAA. So far the prediction was based on tide and persistence of the reminiscent current. Faced with increasing error under changing environmental conditions, further study of other influences became fundamental, in order to increase reliability. This study is a part of that effort by studying the impact of wind-induced currents on forecasting.</p> <p>Based on a year and a half of wind and HF surface current readings, the wind surface current interaction is analyzed and quantified. Then that influence is plugged into the forecast algorithm. The final results show that the wind driven surface current is about 2% of the wind magnitude rotating around 50° clockwise, with coherence after 17h. The wind introduction into the forecast improved the accuracy, but only by an average of 10%. The error still climbs with the variability of the environment, but knowing the wind influence allows other factors' influences to be observed more accurately, such s the magnitude of the current itself. Forecasting is now done with 0.15 m/s plus or minus 0.1 m/s at 95% confidence.</p>			
<b>14. SUBJECT TERMS</b> Surface Current, Wind, HF Radar, Forecast			<b>15. NUMBER OF PAGES</b> 91
			<b>16. PRICE CODE</b>
<b>17. SECURITY CLASSIFICATION OF REPORT</b> Unclassified	<b>18. SECURITY CLASSIFICATION OF THIS PAGE</b> Unclassified	<b>19. SECURITY CLASSIFICATION OF ABSTRACT</b> Unclassified	<b>20. LIMITATION OF ABSTRACT</b> UU

THIS PAGE INTENTIONALLY LEFT BLANK

**Approved for public release; distribution is unlimited**

**THE INFLUENCE OF WIND ON  
HF RADAR SURFACE CURRENT FORECASTS**

Francisco M. S. C. de Almeida  
Lieutenant Commander, Portuguese Navy  
B.S., Escola Naval (Portuguese Naval Academy), 1996

Submitted in partial fulfillment of the  
requirements for the degree of

**MASTER OF SCIENCE IN PHYSICAL OCEANOGRAPHY**

from the

**NAVAL POSTGRADUATE SCHOOL  
December 2008**

Author: Francisco Almeida

Approved by: Jeffrey Paduan  
Thesis Advisor

Curtis Collins  
Second Reader

Jeffrey Paduan  
Chairman, Department of Oceanography

THIS PAGE INTENTIONALLY LEFT BLANK

## ABSTRACT

The ability to predict surface currents can have a beneficial impact in several activities, such as Search and Rescue and Oil Spill Response, as well as others more purely scientific, operational or economic. The Naval Postgraduate School, in conjunction with the Romberg Tiburon Center and the University of California Santa Barbara, has been studying this purpose for the Coastal Response Research Center, University of New Hampshire and NOAA. So far the prediction was based on tide and persistence of the reminiscent current. Faced with increasing error under changing environmental conditions, further study of other influences became fundamental, in order to increase reliability. This study is a part of that effort by studying the impact of the wind-induced currents on forecasting.

Based on a year and a half of wind and HF surface current readings, the wind surface current interaction is analyzed and quantified. Then that influence is plugged into the forecast algorithm. The final results show that the wind driven surface current is about 2% of the wind magnitude rotating around 50° clockwise, with coherence after 17h. The wind introduction into the forecast improved the accuracy, but only by an average of 10%. The error still climbs with the variability of the environment, but knowing the wind influence allows other factors' influences to be observed more accurately, such as the magnitude of the current itself. Forecasting is now done with 0.15 m/s plus or minus 0.1 m/s at 95% confidence.

THIS PAGE INTENTIONALLY LEFT BLANK

## TABLE OF CONTENTS

<b>I.</b>	<b>THE SURFACE CURRENTS FORECAST .....</b>	<b>1</b>
<b>A.</b>	<b>APPLICATIONS .....</b>	<b>1</b>
1.	<b>Navy Type Operations.....</b>	<b>2</b>
<i>a.</i>	<i>Special Operations .....</i>	<i>2</i>
<i>b.</i>	<i>Mine Warfare .....</i>	<i>2</i>
<i>c.</i>	<i>Flag Presence.....</i>	<i>3</i>
<i>d.</i>	<i>Maneuvers and Evolutions .....</i>	<i>3</i>
<i>e.</i>	<i>Weapons Practice.....</i>	<i>3</i>
2.	<b>Coast Guard Type Operations.....</b>	<b>3</b>
<i>a.</i>	<i>Search and Rescue .....</i>	<i>3</i>
<i>b.</i>	<i>Oil Spill Response .....</i>	<i>4</i>
<i>c.</i>	<i>Illegal Traffic and Immigration .....</i>	<i>4</i>
<i>d.</i>	<i>Patrol .....</i>	<i>4</i>
3.	<b>Fisheries .....</b>	<b>4</b>
<i>a.</i>	<i>For Those Who Monitor .....</i>	<i>4</i>
<i>b.</i>	<i>For the Fisherman.....</i>	<i>5</i>
4.	<b>Meteorological/Oceanographic.....</b>	<b>5</b>
5.	<b>Commercial and Recreational Navy .....</b>	<b>5</b>
6.	<b>Habitat Impact .....</b>	<b>5</b>
<b>B.</b>	<b>ACTUAL MODELS .....</b>	<b>5</b>
1.	<b>The Naval Postgraduate School Model.....</b>	<b>6</b>
2.	<b>The Coast Guard / University of Connecticut Model.....</b>	<b>7</b>
<b>C.</b>	<b>FORECAST AND THE INTRODUCTION OF WIND INFLUENCE .....</b>	<b>8</b>
<b>II.</b>	<b>THE WIND / SURFACE CURRENT INTERACTION .....</b>	<b>9</b>
<b>A.</b>	<b>PREVIOUS WORKS USED IN THIS STUDY .....</b>	<b>9</b>
1.	<b>Ekman, 1905 .....</b>	<b>9</b>
2.	<b>McNally, Luther and White, 1988.....</b>	<b>10</b>
<i>a.</i>	<i>The angle .....</i>	<i>11</i>
<i>b.</i>	<i>Correlation .....</i>	<i>11</i>
<i>c.</i>	<i>Major Axis.....</i>	<i>11</i>
<i>d.</i>	<i>Lags.....</i>	<i>11</i>
3.	<b>Foster, 1993.....</b>	<b>11</b>
4.	<b>Xu and Bowen, 1993; Monismith et al., 2006 .....</b>	<b>12</b>
5.	<b>Yelland and Taylor, 1995 .....</b>	<b>12</b>
6.	<b>Ardhuin, Chapron and Elfouhaily, 2003 .....</b>	<b>12</b>
7.	<b>Ullman et al., 2003.....</b>	<b>12</b>
8.	<b>O'Donnall et al., 2005 .....</b>	<b>13</b>
9.	<b>Garfield, Paduan and Ohlmann, 2007 .....</b>	<b>13</b>
10.	<b>Ardhuin et al., October 2008.....</b>	<b>13</b>
<b>B.</b>	<b>DATA .....</b>	<b>14</b>
1.	<b>Winds .....</b>	<b>15</b>
<i>a.</i>	<i>NDBC Buoys .....</i>	<i>16</i>

	b.	<i>MBARI Buoys</i> .....	17
	c.	<i>Resolution and Accuracy</i> .....	17
	d.	<i>Handling</i> .....	18
	e.	<i>Other Series Created</i> .....	18
2.	<b>Currents</b> .....		18
	a.	<i>CODAR Technology</i> .....	19
	b.	<i>CODAR Stations</i> .....	21
	c.	<i>Resolution and Accuracy</i> .....	23
	d.	<i>Handling</i> .....	23
	e.	<i>Other Series Created</i> .....	23
3.	<b>Both Wind and Current</b> .....		24
C.	<b>EMPIRICAL APPROACH</b> .....		24
	1.	<b>Principal Axis (Biggest Variance)</b> .....	24
	2.	<b>Complex Correlation (Kundu, 1975)</b> .....	26
	3.	<b>Scatter Comparison</b> .....	28
	4.	<b>Auto Correlation (McMahan and Wyland, NPS Lab Software, 2007)</b> .....	31
	5.	<b>Power Spectra and Straight Coherence</b> .....	35
	6.	<b>Rotary Spectra (Gonnella, 1972 and Mooers, 1972, Bahr, 2007 Software)</b> .....	37
	7.	<b>Vector Cross Spectral Analysis (Mooers, 1972 and McNally et al, 1989, After Jessen and Bahr, 2007 software)</b> .....	40
D.	<b>THEORETICAL APPROACH</b> .....		42
E.	<b>COMPARISON</b> .....		43
F.	<b>CONCLUSIONS</b> .....		43
	1.	<b>Transfer Function</b> .....	44
	a.	<i>Magnitude</i> .....	44
	b.	<i>Angle</i> .....	44
	2.	<b>Notes</b> .....	44
III.	<b>THE FORECAST</b> .....		45
	A.	<b>FORECAST WITH CODAR</b> .....	45
	1.	<b>Reliability of a Forecast</b> .....	45
	2.	<b>Accuracy of a Forecast</b> .....	45
	B.	<b>PREVIOUS ATTEMPTS</b> .....	46
	1.	<b>Problems</b> .....	46
	2.	<b>Results</b> .....	46
	C.	<b>THE INTRODUCTION OF WIND</b> .....	47
	1.	<b>With Tides Treatment</b> .....	48
	2.	<b>With Persistence</b> .....	51
	D.	<b>TUNING</b> .....	52
	E.	<b>COMPARISON</b> .....	52
	F.	<b>ERROR CAUSES</b> .....	57
	1.	<b>Accuracy Expectancy</b> .....	58
	a.	<i>CODAR (From Wright, 2008)</i> .....	58
	b.	<i>Winds</i> .....	58

c.	<i>Tides (Pawlowicz et al., 2002)</i> .....	58
d.	<i>Growing Surface Waves (Ardhuin et al., 2003)</i> .....	58
e.	<i>Eddy Surface Velocity</i> .....	58
f.	<i>Others</i> .....	58
2.	<b>Abrupt Changes</b> .....	59
IV.	<b>CONCLUSIONS</b> .....	63
A.	<b>THE WIND INFLUENCE</b> .....	63
B.	<b>RESULT CAPABILITIES</b> .....	64
C.	<b>NEXT STEPS</b> .....	64
	<b>LIST OF REFERENCES</b> .....	67
	<b>BIBLIOGRAPHY</b> .....	69
	<b>INITIAL DISTRIBUTION LIST</b> .....	71

THIS PAGE INTENTIONALLY LEFT BLANK

## LIST OF FIGURES

Figure 1.	Ekman Spiral. – The angle between the wind and the surface current is 45° clockwise in the Northern Hemisphere (From: <a href="http://oceanservice.noaa.gov">http://oceanservice.noaa.gov</a> , September 2008). ....	9
Figure 2.	Matching data of Wind and Current – Each jump in the line corresponds to an interval with no data. ....	14
Figure 3.	Current and Wind reading stations – Dots represent one example hourly coverage of the Pescadero CODAR station. (From: ArcGIS. Coastline from NOAA, National Ocean Service, 1994.).....	15
Figure 4.	NDBC type buoy. (From: National Data Buoy Center, <a href="http://www.ndbc.noaa.gov">http://www.ndbc.noaa.gov</a> , October 2008). ....	16
Figure 5.	MBARI M0 and M1 buoys. (From: <a href="http://www.mbari.org">http://www.mbari.org</a> , October 2008)...	17
Figure 6.	Point Sur CODAR station – The receiver antenna is closer and the transmitter further down. (From: CODAR, <a href="http://www.codaros.com">http://www.codaros.com</a> , October 2008). ....	19
Figure 7.	Bragg scattering phenomenon – The biggest return in scattered energy is $\frac{1}{2} \lambda$ (wavelength) of the sea wave. (From: Martin, 2004 in “An introduction to Ocean Remote Sensing,” Cambridge.).....	20
Figure 8.	Bragg scattering phenomenon. Received power by frequency – The difference of where the peak is and where it should be for that particular $\lambda$ , is proportional to the radial current velocity. (From: Paduan & Graber, 1997.) .....	21
Figure 9.	Principal axis analysis – Values correspond to variance and $\alpha$ is the angle between the two full lines. (Monterey station.).....	25
Figure 10.	Complex correlation – Modulus is a measure of correlation and $\alpha$ is the physical angle. (Monterey station.).....	27
Figure 11.	Scattering diagram for U and best fit expression. (Monterey station, Jul 06 to Dec 07.).....	29
Figure 12.	Scattering diagram for V and best fit expression. (Monterey station, Jul 06 to Dec 07.).....	29
Figure 13.	Scattering diagram for Modulus and best fit expression. (Monterey station, Jul 06 to Dec 07.).....	30
Figure 14.	Autocorrelation for Wind – The bottom is a zoom of the first positive 2000h ~ 3 Months. Daily, synoptic and monthly oscillations are present. (Monterey station, Jul 06 to Dec 07.) .....	32
Figure 15.	Autocorrelation for Current – The bottom is a zoom of the first positive 2000h ~ 3 Months. Daily, synoptic and monthly oscillations are present. (Monterey station, Jul 06 to Dec 07.) .....	33
Figure 16.	Autocorrelation for Current with tides removed – The bottom is a zoom of the first positive 2000h ~ 3 Months. Daily, synoptic and monthly oscillations are present. (Monterey station, Jul 06 to Dec 07.).....	34
Figure 17.	Power spectra of Wind and Current – Dashed at 95% confidence. (Monterey station, Jul 06 to Dec 07.) .....	35

Figure 18.	Power spectra of Wind and Current with tides removed – Dashed at 95% confidence (Monterey station, Jul 06 to Dec 07.).....	36
Figure 19.	Coherence and Phase between wind and current – Dashed at 95% confidence. (Monterey station, Jul 06 to Dec 07.).....	37
Figure 20.	Rotary components for wind – Notice the two peaks for 12 and 24h. (Monterey station, Jul 06 to Dec 07.) .....	37
Figure 21.	Rotary components for current, tides in and out – Notice a small decrease in energy. (Monterey station, Jul 06 to Dec 07.) .....	38
Figure 22.	Rotary coefficient for Wind – A fully rotational movement would be valued 1. (Monterey station, Jul 06 to Dec 07.).....	39
Figure 23.	Rotary coefficient for Current, tides in and out. (Monterey station, Jul 06 to Dec 07.).....	39
Figure 24.	Complex Coherence and Phase – Lower image is a zoom of the coherent part. (Monterey station, Jul 06 to Dec 07.) .....	40
Figure 25.	Complex coherence and Phase, tide removed – Top, all constituents. Bottom, all constituents removed but S1. (Monterey station, Jul 06 to Dec 07.) .....	42
Figure 26.	Results for RMS compared with wind and number of pseudo drifters – RMS for 24h. The number of pseudo drifters present may be used as a proxy for current speed. (Image from Garfield et al., 2007.).....	47
Figure 27.	Basic flow chart diagram of the forecast procedure – Several adaptations were attempted. ....	48
Figure 28.	One day forecast with tide treatment – The wind changing its influence. (Monterey Station.).....	50
Figure 29.	One day forecast with persistence – The wind changing its influence. (Monterey station.).....	51
Figure 30.	The difference between winds – Several positions of the future wind interval were attempted for a given time of prediction ( $t_p$ ).....	52
Figure 31.	Relation of RMS error and the stations – Top is magnitude of the current vs. error. Bottom is variability vs. error. Based on the tide plus mean with transfer function model forecasts.....	54
Figure 32.	Relation of RMS error and seasons – Top is magnitude of the current vs. error. Bottom is variability vs. error. (For Monterey station, based on the tide plus mean wind transfer function forecasts.) .....	55
Figure 33.	Zoom of a plot with the different calculated RMS – Wind influence. “p” is persistence, “nw” is no wind. (Monterey station.).....	56
Figure 34.	Zoom of a plot with the different calculated RMS – Possible tide problem. “p” is persistence, “nw” is no wind. (Monterey station.).....	57
Figure 35.	Full RMS plot versus SWH, current and wind. (Monterey station, Jul 06 to Dec 07.).....	60
Figure 36.	Zoom of RMS versus SWH, current and wind – High error seems associated with large current variation. Top with tides treatment. Bottom with persistence. (Monterey station.).....	61

## LIST OF TABLES

Table 1.	NDBC Buoy (From: National Data Buoy Center, <a href="http://www.ndbc.noaa.gov">http://www.ndbc.noaa.gov</a> , October 2008.).....	16
Table 2.	MBARI Buoy (From: Monterey Bay Aquarium Research Institute, <a href="http://www.mbari.org">http://www.mbari.org</a> , October 2008; Depths (From: ICON, <a href="http://www.oc.nps.edu/~icon/moorings">http://www.oc.nps.edu/~icon/moorings</a> , November 2008).....	17
Table 3.	CODAR stations (From: <a href="http://www.cencalcurrents.com">http://www.cencalcurrents.com</a> , September 2008.).....	22
Table 4.	Principal axis analysis. – Values correspond to magnitudes and angle between the major axis and north. (Monterey station.) .....	25
Table 5.	Principal axis analysis. – Space and time variability (wind – current.).....	26
Table 6.	Complex correlation. – Space and time variability.....	28
Table 7.	Best fit expression. – Space and time variability.....	31
Table 8.	Added variances ~ energy. (Monterey station.).....	36
Table 9.	Wind and Current shifting of angles in time. (Averages for all the stations and periods.).....	41
Table 10.	Detidal errors with 3 days and 1 Month data – The calculation of the Root Mean Square error will be discussed in III. E. (Monterey Station.) .....	49
Table 11.	Root Mean Square comparison – Average daily values. (Monterey station, Jul 06 to Dec 07.).....	53

THIS PAGE INTENTIONALLY LEFT BLANK

## LIST OF ACRONYMS

CODAR	Coastal Ocean Dynamics Application Radar
EMR	Electromagnetic Radiation
GDOP	Geometric Dilution of Precision
MBARI	Monterey Bay Aquarium Research Institute
NDBC	National Data Buoy Center
NOAA	National Oceanic and Atmospheric Administration
NPS	Naval Postgraduate School
RMS	Root Mean Square
SAR	Search And Rescue
SAROPS	SAR Optimal Planning System
SST	Sea Surface Temperature
STPS	Short Term Prediction System
SWH	Significant Wave Height

THIS PAGE INTENTIONALLY LEFT BLANK

## ACKNOWLEDGMENTS

The author would like to acknowledge the support of NOAA/UNH's Coastal Response Research Center at the University of New Hampshire.

The author would also like to express his gratitude and appreciation especially to Professor Jeffrey Paduan and Oceanographers Mike Cook and Fred Bahr, who patiently guided and facilitated all the work, and Professor Curt Collins who was so kind to be the second reader. I would also like to thank the Oceanography Department faculty of NPS, who encouraged the work and added so much to my understanding:

Professors	Mary Batteen Peter Chu Ching-Sang Chiu Thomas Herbers
Associate Professor	Timour Radko
Assistant Professor	Jamie MacMahan
Senior Lecturer	Arlene Guest
Research Associate	John Joseph
Oceanographers	Chenwu Fan Paul Jessen Terry Rago
Superv. Gen. Eng.	Robert Wyland

I also appreciate the Oceanography and Meteorology/Oceanography students from 2007/08, with whom so many questions were debated.

Finally, my wonderful wife, Cidália, is the Muse that always pushes me further and further ahead.

THIS PAGE INTENTIONALLY LEFT BLANK

# **I. THE SURFACE CURRENTS FORECAST**

## **A. APPLICATIONS**

The use of the sea is not natural to man. Instead of moving with a solid surface underneath his feet and an almost intangible fluid surrounding him, at sea he has to deal with a much more viscous fluid. One of the major differences that this produces is that on earth, if he stops moving his body, or his car, he stops. At sea, he does not. In order to take the best advantage of this distinction, understanding how this movement works is necessary. In the fifteenth and sixteenth centuries, the Portuguese voyages of discovery that navigated the entire globe in simple sailing ships relayed much of this knowledge. Charts of currents were drawn and pilots were written in each trip.

With the passage of four centuries, several approaches have evolved to face the challenges of today. One of them is the remote evaluation of the surface current by HF RADAR (explained more in detail on II.B.2.a.). This method is excellent in filling the gap between satellite remote sensing measurements and the shore; however, it is not good for the Surf zone, for which other methods can be applied, like the one described in Puleo et al., 2002. Depending on the frequency, HF radar can be used to read from around 3 to 200 km off the coast. Surface currents are obtained with regular readings through this means, allowing the creation of a real time surface picture. Several works are still debating the accuracy of this system and what influences it. This study, focused on the forecast of the next 24 hours (24h) surface currents, takes the next logical step. Extracting currents using electromagnetic radiation (EMR) on the HF band implies that all the readings made are of the first two meters (2m) of depth, because EMR does not reach any further down and in this shallow layer, wind is considered to be a major driver of the currents.

There are not many studies considering the interaction between the previously mentioned surface layer currents and wind, being almost all based on short time series and with limited resolution, most under the inertial period (24h). The existence of a database of two time series of both wind and current, with lengths over one year and with

an hourly resolution, presents an opportunity to unveil some properties of that interaction that are currently poorly known. Based on these time series data (described in II.B.), this thesis's aim is to first find the surface current component that is driven by the wind, by constructing a transfer function between them (described in Section II). This transfer function will then be used as an extra input for an already existing forecast model that relies solely on persistence and tides (described in I.B.), expecting to bring better accuracy and reliability to it. The results obtained for the wind/surface current interaction in this long time series may also be applied to many other future studies.

Due to its practical implications, several institutions are interested in systems that allow this knowledge of the surface currents and in its forecast, because it has direct impact to every sea user that needs to plan any type of short term deployment. That is the case of the National Oceanic and Atmospheric Administration (NOAA) Coastal Response Research Center, who funded a study on "Delivery and Quality Assurance of Short-Term Trajectory Forecasts from HF Radar Observations," of which this thesis is also a part. Better knowledge of the next 24h surface currents may be used to get better results in:

### **1. Navy Type Operations**

Surface current forecasting has a significant impact on non-motorized activities, because propulsion reduces the dependency on the flow to which the user is exposed.

#### ***a. Special Operations***

Deployment of divers or any type of raft maneuvering at the coast may benefit from a shortened mission time and energy, reducing risks and costs.

#### ***b. Mine Warfare***

Locating the positions of drifting mines remains a modern reality because mines are still the cheapest and most effective way of making constraints to the use of a certain sea area or a harbor. To avoid or to sweep drifting mines, knowing where a field

is today will not help much tomorrow, because the mines drift with the current at their depth. If you are deploying, you need to know if the mine behavior will be what you intend.

*c. Flag Presence*

Most flag presence missions consist of long periods where a ship is constrained to a certain position or box. Taking advantage of the currents will result in better efficiency in the use of time and fuel.

*d. Maneuvers and Evolutions*

To maneuver a ship a long distance, the vector of her self propelled velocity must be added to the surface current velocity, also resulting in better efficiency in the use of time and fuel.

*e. Weapons Practice*

Target drift in time.

In live surface fire practice, usually a target is deployed or towed at a very slow speed. More accurate knowledge of the current will predict target drift over time, allowing a better residence time in the exercise area with fewer maneuvers, making it safer.

**2. Coast Guard Type Operations**

*a. Search and Rescue*

Most distressed platforms do not have, or only have partial, locomotion capability. Examples are man overboard, life saving rafts, debris or a damaged ship. Having the correct surface current scenario will allow two major advantages:

(1) Reduces Position Uncertainty to the Distressed Position. The future target position is a function of time multiplied by the elements' influence. When the rescue craft reaches the search zone, it usually has to face an area which size depends on the uncertainty of the surface current and the wind influence on the target

(and the initial position error). Reducing surface current uncertainty will directly reduce the search area, reducing the time needed to find the target, allowing better survivability odds.

(2) Rescue Missions Savings in Hours and Fuel. Added to the advantage in (1) of facing a shorter area, rescuers are able to plan a more accurate intercept course, arriving earlier than possible previously which results in an even tighter search area. On the scene, better sweeping plans can be made.

***b. Oil Spill Response***

Knowledge of the impact area, where a spill occurred and where it is going, allows the efficient deployment of the available means, reducing damage. For a good result, it must be coupled with the pollutant's dispersive characteristics. Also, it helps track pollutants that may have come from tank washings.

***c. Illegal Traffic and Immigration***

Much of this traffic is done by small slow boats, for which the surface current is a determinant of the true course. Also, sometimes packages are sent adrift on purpose or to avoid capture. Knowing the currents will facilitate the collection of them.

***d. Patrol***

Better efficiency in the use of time, fuel and area covered.

**3. Fisheries**

***a. For Those Who Monitor***

One typical periodic problem is the understanding of how a bloom will spread out. Knowing more about buoyant behaviors helps avoid the capture and consumption of organisms that may have toxic elements. Also, surface current knowledge gives a better understanding of the probable paths of buoyant (or slow velocity) organisms, such as eggs, larvae or youngsters.

***b. For the Fisherman***

Coastal fishermen depend a lot on timing and their profits depend a lot on fuel consumption. The knowledge of how the currents will behave provides a tool to make transits and staying with fisheries' spots more cost efficient. They also benefit from more accurate knowledge of the species behavior described in the previous paragraph.

**4. Meteorological/Oceanographic**

Other than the direct relevance, it is an important tool to models, as they need periodic assimilation of reality data to be accurate. This means can also control model forecasts' quality by direct comparison with its own.

**5. Commercial and Recreational Navy**

Coastal transits can be planned to be more efficient in terms of fuel, time and safety.

**6. Habitat Impact**

Knowledge of buoyant behaviors makes it possible to understand the behavior of an atypical discharge from a river or sewer system, providing a tool to better manage the situation.

**B. ACTUAL MODELS**

Surface currents are usually collected by direct measurements using current meters or current profilers, or by remote sensing systems, such as coastal radars or satellites. In order to make forecasts, there is need of actual observations plus a model for future behavior, and forecasting ability will be in direct relation to the type of observations available.

Retrieved data from satellite remote sensing is usually based on readings of sea surface temperature (SST), or other pixel differentiation information, to allow tracking of characteristics by maximum cross correlation. This gives resolutions good enough for coastal applications that range from 1 km to 25 km according to the frequency used, the latter for microwave, which is the only method able to penetrate clouds (Emery et al.,

2005). They are then coupled with satellite altimetry information to create the geostrophic flow and make corrections, if a satellite is already on task. However, there are two primary disadvantages to using satellites: they are more expensive to operate and have less time resolution, despite the possibility of coupling with models in between. Since the time resolution is twice a day, a function of the orbit, it does not allow handling of smaller time scale phenomena. Those phenomena may not be very important in the open sea, but they gain substantial, if not major, influence near shore. One of such cases is the tides. Also, tides cannot be forecasted with poorer resolutions. No quantitative evaluation of the accuracy of these models was found in the references.

The use of radar systems for this purpose is becoming widely used throughout the world because of the many unique applications that exist for real-time surface current mapping data. Also, it is a cheaper and less dependent system compared with the use of satellites, particularly if the user is interested primarily in coastal currents. Since the real time data is already collected, several academic, operational and commercial institutions have been trying to go further and forecast the surface currents. Following are descriptions of two models referencing this work.

### **1. The Naval Postgraduate School Model**

This approach relies on the Coastal Ocean Dynamics Applications Radar (CODAR – a HF RADAR system) readings of surface currents, as described in II. B. 2. a.. These readings are then treated for Geometric Dilution of Precision (GDOP), which takes into account the uncertainty provoked by the angle of the azimuths between stations and reading position (the closer to 90 degrees, the better). The currents associated with tides are then removed by software from *MathWorks* called “t\_tide.” More information about “t\_tide” can be found in Pawlowicz et al., 2002, which performs a best fitting frequency relation between the time series and the tidal harmonic constituents, taking the period of interest into account. This model uses a Cook, 2008, alteration to the software. After removing the tidal effects from the current, the remaining current is then averaged to the mean current for that day. Based on persistency, this current is then projected to the next 24 hours and is added to the tidal current that is again forecasted by the “t\_tide”

prediction software. The accuracy of this model is typically 7km distance after 24h, but frequently exceeds 20km.( Garfield et al., 2007). This thesis builds on this model improvement by introduction of the wind influence.

## **2. The Coast Guard / University of Connecticut Model**

Working with the U.S. Coast Guard, the University of Connecticut developed the Short Term Predictive System (STPS, Ullman et al., 2003; O'Donnell et al., 2005) for the U.S. Coast Guard Research & Development Center. This model also relies on CODAR readings treated for GDOP. In their work several essays were attempted. In the last, the surface current was divided into three parts: tidal flow, wind driven and mean. The tides and the wind influence are estimated by a different algorithm, the Gauss-Markov estimator, which divides what part of a signal is tidal or wind motivated and what is not, by comparison of time series, creating weights that are calculated from the autocovariance functions. This signal decomposition then allows prediction of the next 25h by persistence, tide and predicted winds influence. One NDBC buoy is used for the wind data, with results more accurate than those from the previous Coast Guard results using only NOAA's tidal data. Root Mean Square (RMS) errors were in the order of 10 cm/s (ten centimeters per second) for each component of the velocity, u and v (corresponding to 14.14 cm/s for the vector). Forecasts for search boxes were then made with 20 cm/s RMS in order to cover uncertainty in all measurements and then compared with real data from drifters and statistical approaches by a Monte Carlo simulation.

The main differences between the Coast Guard model and the one used in this thesis are: the length of the evaluation data set – seven days versus 1,5 years, the way the estimation for the tides and winds influences are calculated – Gauss Markov during one Month for the tides and during 1 day for the wind versus  $t_{\text{tide}}$  for one Month and time series analysis for 1,5 years respectively, the wind data position (number of buoys) – one versus five different positions, and the different number of CODAR data stations – two versus 10 different stations. The STPS concludes that “...another analysis approach to quantifying the wind-driven circulation is called for.”

### **C. FORECAST AND THE INTRODUCTION OF WIND INFLUENCE**

All the works concerning forecast of surface currents point to the necessity of accurately knowing all its dependencies and their magnitudes. We know that the end result will be in direct proportion to the accuracy of the data and of the relations we plug in. One of those dependencies is the wind, as Ekman's work proved by taking one step further our intuitive experience that the wind influences the movement of the water underneath it (Ekman, 1905).

The work reported here was done after the initial results of the use of the Naval Postgraduate School model for the NOAA's Coastal Response Research Center (Garfield et al, 2007), where the need to understand the wind's influence on the surface current was identified as possibly relevant, among other factors. Despite this thesis's focus on the wind, other dependencies will also be analyzed when doing error assessment. In order to reach a forecast model including the wind, a full time-series analysis study of wind / surface current interaction is made and shown in section II. After detailing this interaction, and having a transfer function created, a forecast model is put to work producing results, which will be described in Section III. Conclusions from these results are then extrapolated and discussed in Section IV.

## II. THE WIND / SURFACE CURRENT INTERACTION

### A. PREVIOUS WORKS USED IN THIS STUDY

Despite the long list of studies on air / sea interaction, few studies were found concerning strictly the interaction between the wind and the surface current, with quantified results for periods less than 24 hours. Nevertheless, portions of the following works contribute to the understanding of the wind surface current relation process:

#### 1. Ekman, 1905

Although this thesis is based on mainly empirical results, Ekman provided the basic theoretical support for it (Ekman, 1905). Starting with the geostrophic equations with vertical friction and dividing the flow into geostrophic and frictional components, he related the wind stress and its influence on the oceanic flows as a function of depth, creating, among other results, what we now know as “Ekman Spiral” (Figure 1). The Ekman theory assumes infinite ocean and constant eddy viscosity ( $A_v$ ), which is an approximation of an already poorly known value (Radko, NPS class notes, 2007).

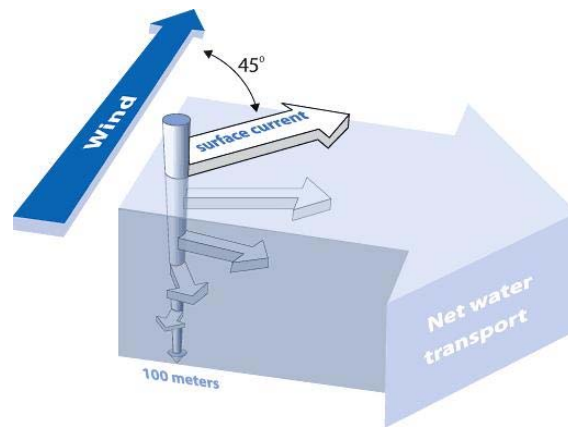


Figure 1. Ekman Spiral. – The angle between the wind and the surface current is  $45^\circ$  clockwise in the Northern Hemisphere (From: <http://oceanservice.noaa.gov>, September 2008).

According to his work, the wind stress is given by:

$$\vec{\tau} = \rho_0 A_v \frac{\partial \vec{v}}{\partial z} \quad (1)$$

where  $\tau$  is the wind stress and  $\rho_0$  represents the water density as a constant.

The amplitude in depth is

$$|\vec{v}_E| = |\vec{v}_0| e^{\sqrt{\frac{f}{2A_v}} z} \quad (2)$$

f being the Coriolis term and z the depth.

The direction is shown by:

$$\varphi = \sqrt{\frac{f}{2A_v}} z + \varphi_0 \quad (3)$$

$\varphi_0$  being the angle at the surface.

For this study, the two main results are:

- The angle of the current at the surface, which is 45° to the right of the wind stress.
- The amplitude of the velocity shown by

$$|\vec{v}_{0E}| = \frac{|\vec{\tau}_0|}{\rho_0 \sqrt{A_v f}} \quad (4)$$

## 2. McNally, Luther and White, 1988

This is a study on subinertial frequency response of wind driven currents in the mixed layer. The data set consisted of 63 tracks of drifters, between 1976 and 1981, with results being binned at 5 days periods. The drifters operated at a 30m depth. The study described a process of the interaction between wind and currents, despite the different objective, analyzed depth and periods. Among the results are descriptions of the following effects indirectly related to this work.

*a. The angle*

The angle was found to be around 25° to the right of the wind stress (at 30m), which means the existence of the clockwise rotation in depth, despite the angle, was smaller than the expected by Ekman theory.

*b. Correlation*

The correlation was found to be significant between near inertial to 16 days. No relation was found under the inertial period.

*c. Major Axis*

This was found to be from 75° to the right of the wind stress at near inertial to 15 ° at the lower frequencies.

*d. Lags*

Lags were observed from 30 ° at near inertial to zero, corresponding to under four hours in time.

**3. Foster, 1993**

This thesis studied the relation between diurnal surface winds and currents in Monterey Bay. The author analyzed the daily wind surface relation for September 1992 in Monterey Bay, using two CODAR sites for the currents, two moorings and three coastal stations for the winds. The result was data on the behavior of the wind and current circulation and interaction in this zone of the Monterey Bay. The major results that impact this study are the current response to the breezes be under two hours (the time resolution of the data) and the fact that the more offshore currents rotate clockwise in time, to the right of the wind.

#### **4. Xu and Bowen, 1993; Monismith et al., 2006**

This is a work on wave and wind driven flow interaction. From this study, the major contribution is the description of an Eulerian return flow (Hasselmann's drift) that cancels the Stokes drift, allowing for a measure of the uncertainty related to the waves' influence on the currents.

#### **5. Yelland and Taylor, 1995**

This is a work on wind stress measurements from the open ocean. The values of the drag coefficient ( $C_D$ ) for the theoretical approach made in II.D. are used according to this study's conclusions:

- For winds speeds at 10 m ( $U_{10}$ ) from 3 to 6 m/s

$$1000C_D = 0.6 + 0.07U_{10} \quad (5)$$

- For winds speeds at 10 m from 6 to 26 m/s

$$1000C_D = 0.6 + 0.07U_{10} \quad (6)$$

#### **6. Ardhuin, Chapron and Elfouhaily, 2003**

This is a work about the interaction between wind and waves. The result of this study that most contributes to this thesis is that for growing waves in short fetches, there is a wave induced stress that opposes the wind stress, consuming up to 10% of the energy. This directly influences the transfer function and the forecast that, practically, is only based on actual currents and wind forecast. To remove this influence, a measure of the wave height difference due to wind presence should be introduced – which it self is a function of magnitude and direction of the wind and of the waves height, wavelength and direction and of the fetch.

#### **7. Ullman et al., 2003**

These authors prepared a for the United States Coast Guard, Department of Homeland Security, on the use of CODAR technology in Search and Rescue (SAR) planning. This work was continued by the next study referenced.

## **8. O'Donnall et al., 2005**

This is also a study prepared for the United States Coast Guard, Department of Homeland Security, on the integration of CODAR and a Short-Term Predictive System (STPS) surface current estimate into the Coast Guard's SAR Optimal Planning System (SAROPS). This study is a catalyst and at the same time a measure of comparison for the results of this thesis. As described in I.B.2., its goals and approach were the same, but used more limited data and a different mathematical analysis. One of its conclusions mentioned the necessity of a work such as this thesis. This thesis results ended up being similar.

## **9. Garfield, Paduan and Ohlmann, 2007**

A report prepared for the Coastal Response Research Center, this is a study funded by NOAA and the University of New Hampshire. One of the focuses of this report was to test the accuracy of the Naval Postgraduate School model, and it pointed to the necessity of studying the other interactions, starting with the wind. For this purpose, a comparison is made between CODAR forecasted positions and CODAR reading positions of simulated drifters after 24h. Its conclusions mention that "one environmental factor that is expected to play a role is wind," despite inconclusive results. The study also mentions that there is "some connection between strong currents (...) and large RMS separation."

This thesis is an active part of the continuation of this work.

## **10. Arduin et al., October 2008**

This study came to the attention of the author during the writing stage of this thesis. Coincidentally, it concerned exactly the focus of section II: the inducing of currents by the wind. Its conclusions bolster the ones reached in this thesis, having points in common such as the magnitude of the wind driven current measured around 2% and the angle between the velocity vectors observed from 10 to 40 degrees, based on a two-

year time-series analysis. Moreover, the study goes further in theorizing about the wave's influence, one of this thesis's proposals for necessary future work, as pointed to by II.A.4. and II.A.6.

## B. DATA

As mentioned earlier, this work is one of the first able to study two long reliable time series, with continuous one hour measures for more than one year. All data analyzed was gathered from June 1, 2006 to December 31, 2007. Figure 2 shows the time intervals for each station. This allows a wide spectrum of possibilities and test scenarios in space and time, as well as providing outputs of the time series analysis with a very good resolution, maintaining a continuous information flow with a high confidence level. Current data is gathered from 10 CODAR stations, with calculations of currents for five NDBC buoys positions, from where the wind data are obtained (Figure 3).

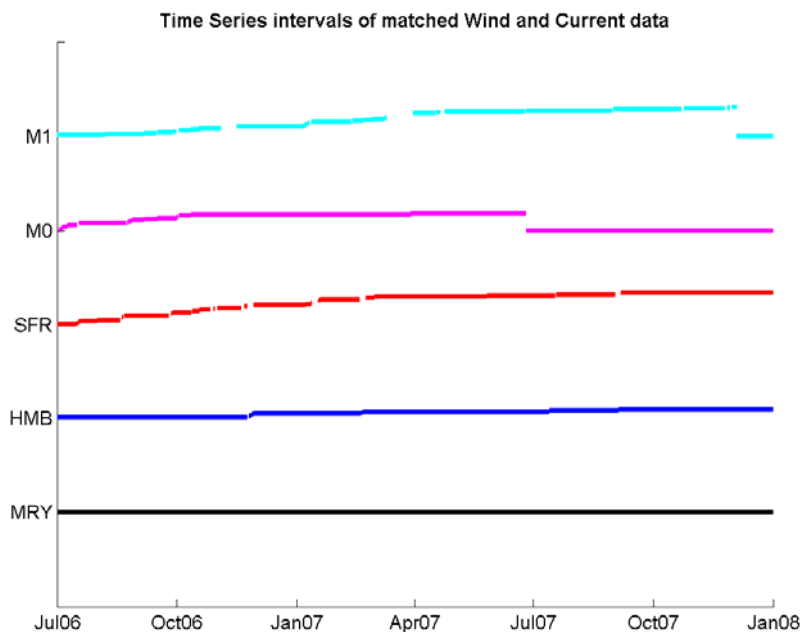


Figure 2. Matching data of Wind and Current – Each jump in the line corresponds to an interval with no data.

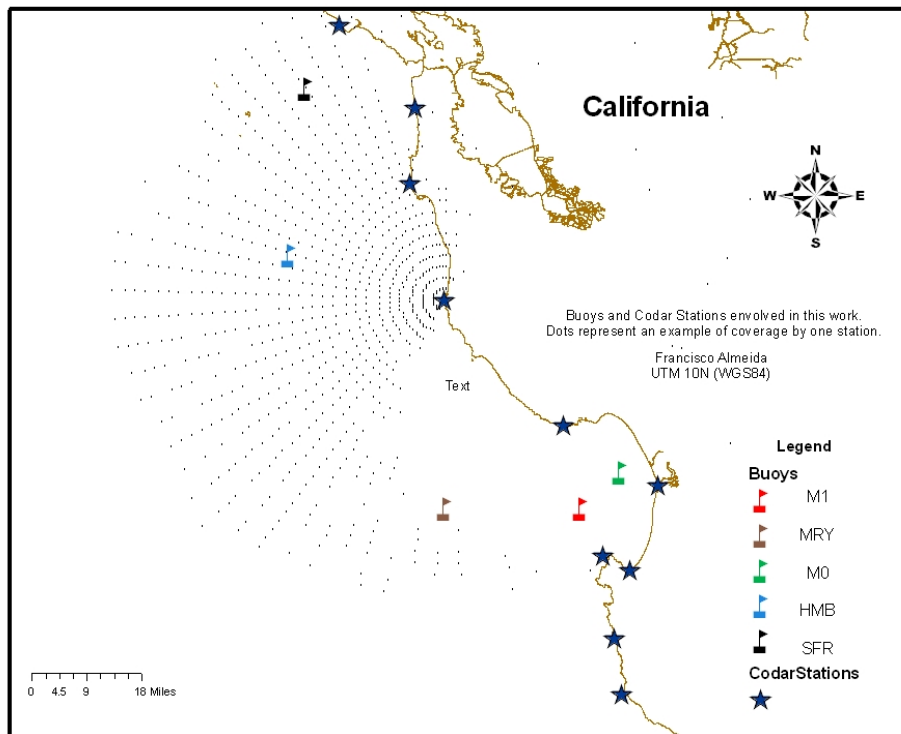


Figure 3. Current and Wind reading stations – Dots represent one example hourly coverage of the Pescadero CODAR station. (From: ArcGIS. Coastline from NOAA, National Ocean Service, 1994.)

### 1. Winds

Winds were obtained from NOAA's National Data Buoy Center (NDBC; Figure 4, Table 1), and from the Monterey Bay Aquarium Research Institute (MBARI; Figure 5, Table 2) moored buoys.

a. *NDBC Buoys*



Figure 4. NDBC type buoy. (From: National Data Buoy Center, <http://www.ndbc.noaa.gov>, October 2008).

Data from the following NDBC buoys / stations is used:

#	Name	Distance to shore	Type	Position	Elevation	Anemometer height	Water depth	Watch circle radius
46012	Half Moon Bay (HMB)	4 NM	3 m discus	37.361N 122.881W	sea level	5 m	213.1 m	170 yds
46026	San Francisco (SFR)	18 NM	3 m discus	37.759N 122.833W	sea level	5 m	52.1 m	127 yds
46042	Monterey (MRY)	27 NM	3 m discus	36.753N 122.423W	sea level	5 m	2115 m	2175 yds

Table 1. NDBC Buoys (From: National Data Buoy Center, <http://www.ndbc.noaa.gov>, October 2008.)

**b. MBARI Buoys**



Figure 5. MBARI M0 and M1 buoys. (From: <http://www.mbari.org>, October 2008).

Data from the following MBARI buoys / stations is gathered from:

Name	Position	Elevation	Anemometer height	Water depth
M0	6.835N 121.899W	sea level	4 m	70 m
M1	36.750N 122.020W	sea level	4 m	1000 m

Table 2. MBARI Buoys (From: Monterey Bay Aquarium Research Institute, <http://www.mbari.org>, October 2008; Depths (From: ICON, <http://www.oc.nps.edu/~icon/moorings>, November 2008).

Notice that since M0 and M1 are well inside the Monterey Bay (Figure 5), their data differ from the other's positions because they are under the control of the typical Bay circulation and winds, of high topographic and land influence.

**c. Resolution and Accuracy**

The resolution of the anemometers is unknown but the readings are valued to 0.0001 m/s. The accuracy is also unknown, but considering the readings' detail, variance is considered to be small.

*d. Handling*

In order to enable treatment and comparison among different equipment readings, all the data must be formatted into a similar shape. Therefore, all of the wind time series are:

- Hourly averages of the available 10 minute readings, from the exact hour - 30 min to + 30 min;
- Arranged in the form of a three dimensional vector of time (in hours), u velocity (seasonal, in m/s) and v velocity (meridional, in m/s);
- Interpolated for gaps under 6 hours;
- arranged so that seasonality, monthly, synoptic and daily influences are studied by subdivisions of the series in intervals of three months, one month, six days and one day.
- calibrated such that spatial influence is studied by the different locations.

*e. Other Series Created*

A different time-series is also created for the wind readings of the Monterey and Half Moon Bay NDBC buoys, where the y axis is rotated for the winds' largest variance azimuth, maintaining the x axis in perpendicular alignment. This will serve to interpret the angle between the two major variances of wind and current, extracting conclusions on interaction both for rotated axis for wind biggest variation only and for wind data rotated for the wind biggest variation and current to the current biggest variation.

**2. Currents**

Currents were obtained from all the in-range CODAR stations, for all the positions of the wind stations mentioned in the previous section from the buoys positions. A photograph of a typical CODAR transmit and receive antenna configuration is shown in Figure 6. Despite the increasing number of CODAR stations around the world, there have not been many opportunities to operate for a long period with so many stations in a single study, increasing the number of radial readings for each position. A short explanation of how CODAR technology appeared and operates is given in paragraph a.

a. *CODAR Technology*



Figure 6. Point Sur CODAR station – The receiver antenna is closer and the transmitter further down. (From: CODAR, <http://www.codaros.com>, October 2008).

CODAR consists of radar in the HF band, which is the band that corresponds to wavelengths of the same magnitude of the sea waves. The first correlations between radar and waves appeared accidentally at the end of the Second World War, when echoes appeared in near shore radar stations. In 1955, “Crombie discovers experimentally that Bragg scatter produces strong HF sea echo” (CODAR, <http://www.codaros.com>, October 2008).

CODAR uses the Bragg Scattering phenomenon (Figures 7 and 8) to measure the wavelength of the sea waves that are approaching or going away, in a radial direction, to each station. Having the wavelength, we calculate the speed a wave should have from the deep water dispersion relation. The difference of where the received frequency peak is and where it should be in that particular wavelength is a measure of the radial surface current by (Doppler, 1803-1853):

$$f' = f_0 \frac{1}{1 + \frac{v}{c_0}} \quad (7)$$

$f'$  being the new peak frequency,  $f_0$  the expected peak with no current,  $v$  the radial current velocity and  $c_0$  the theoretical velocity of a wave with that wavelength in deep water. With two of these measurements, if properly intercepting, we obtain the two components of the velocity vector.

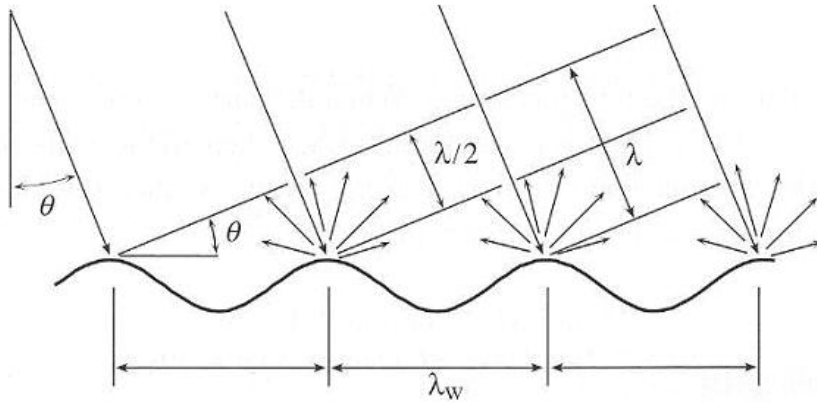


Figure 7. Bragg scattering phenomenon – The biggest return in scattered energy is  $\frac{1}{2} \lambda$  (wavelength) of the sea wave. (From: Martin, 2004 in “An introduction to Ocean Remote Sensing,” Cambridge.)

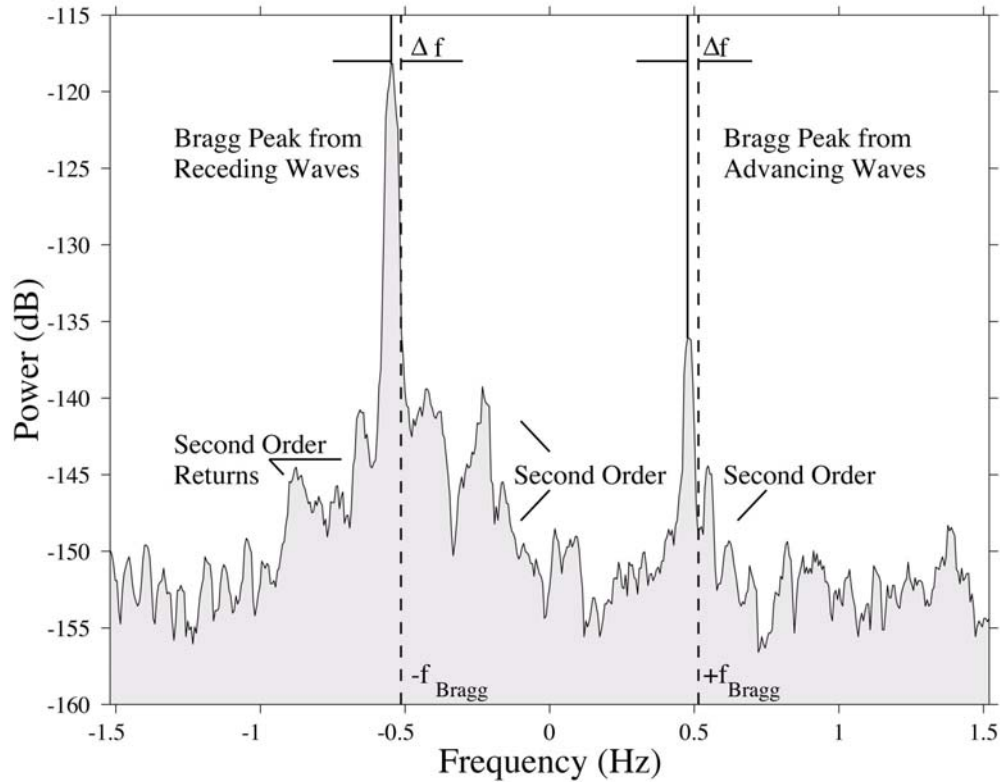


Figure 8. Bragg scattering phenomenon. Received power by frequency – The difference of where the peak is and where it should be for that particular  $\lambda$ , is proportional to the radial current velocity. (From: Paduan & Graber, 1997.)

For the frequencies used in these stations, the measurements are related to the first one meter of the water column; horizontally, the result for a single observing bin is based on backscatter from, approximately, 3 x 3 km of surface area.

### ***b. CODAR Stations***

All stations but the one off Moss Landing consisted of a standard 11.5-14 MHz apparatus; Moss Landing operated in the range 24-27 MHz. Their approximate positions (in Geographic Coordinate System) are given in Table 3.

<b>CODAR station</b>	<b>Position</b>
Commonwheel	37.911833N 122.728167W
Fort Funston	37.712050N 122.5013W
Montara	37.533717N 122.519217W
Pescadero	37.252483N 122.416567W
Santa Cruz	36.949217N 122.0661W
Moss Landing	36.803667N 121.787917W
Point Pinus	36.636783N 121.9536W
Naval Postgraduate School	36.603333N 121.87195W
Granite Canyon	36.439450N 121.922217W
Point Sur	36.305767N 121.90125W

Table 3. CODAR stations (From: <http://www.cencalcurrents.com>, September 2008.)

*c. Resolution and Accuracy*

The resolution for these stations is 0.04 m/s (from <http://www.codaros.com>, accessed in October 2008). The most recent studies show accuracy from 8 to 18 cm/s (from Wright, 2008, NPS Masters Thesis).

*d. Handling*

In order to be able to work with these time series all the data have to be arranged in a similar fashion. All of the current time series are:

- Hourly averages from the exact hour -30 min to + 30 min, interpolated from the nearest valued positions to the buoys position. This is the way the data is presented by the CODAR system.
- Arranged in the form of a three dimensional vector of time (in hours), u velocity (seasonal, in m/s) and v velocity (meridional, in m/s). This arrangement allows easy handling.
- Interpolated for gaps under 6 hours. This allows a good continuity and guarantees no hiding of important features in the changing of the current.

*e. Other Series Created*

Other time-series were also created for the current readings of the position of the Monterey and Half Moon Bay NDBC buoys:

- Where the y axis is rotated for the wind's largest variance azimuth, maintaining a perpendicular x axis;
- Where the y axis is rotated for the current's largest variance azimuth, maintaining a perpendicular x axis. (Comparison of the results from steps (1) and (2) also provides information about the most common angle between surface current and wind.)
- All the series created for the Monterey buoy have two more associated scenarios, where the tide influence from the current is tentatively removed. For this purpose the software t\_tide is used (Pawlowicz, Beardsley and Lentz, 2002 with a Cook, 2008, alteration to the software). In the first, all of the tide constituents available in the software are used, once this time-series is long enough (in this case, one and a half years). In the second one, all but the S1 constituents are used, in order to avoid removing the sea breeze influence. In both we have to take into account that the energy removed may not be just tide related, as occurs in periods of the order of the rotation of the planet's rotation frequency.

- Seasonality, monthly, synoptic and daily influences are studied by subdivisions of the series in intervals of three months, one month, six days and one day.
- Spatial influence is studied by the different locations.

### **3. Both Wind and Current**

The time series of both wind and current are then cut in order to create time intervals where they both exist, to make comparison possible. The resulting matched intervals are displayed in Figure 2.

From now on in this thesis, for reference simplicity, when a station is mentioned by place name it refers to the buoy position; e.g., “Monterey Station” means the data obtained for the position of the 46042 NDBC buoy. Because the Monterey station has a broader continuous time series, it allows us to extrapolate more results with a better resolution. That particular location is where most studies and essays are made, the others serving as comparisons.

## **C. EMPIRICAL APPROACH**

Two independent paths are taken. The first starts with real data and tries to extrapolate relations from it. This approach relies on pure Time Series Analysis. The second, described in II D., is based on theoretical knowledge and serves as comparison to the empirical results.

All of the following methods are applied in all of the time series described in B.

### **1. Principal Axis (Biggest Variance)**

The objective is to have a measure of the axis which experiences the largest variance and its angle of measurement, for both wind and current. The result is plotted as Figure 9 and as a table in Table 4, where the two major semi-axes in the along vector direction are shown in full (using Bahr, 2007, software):

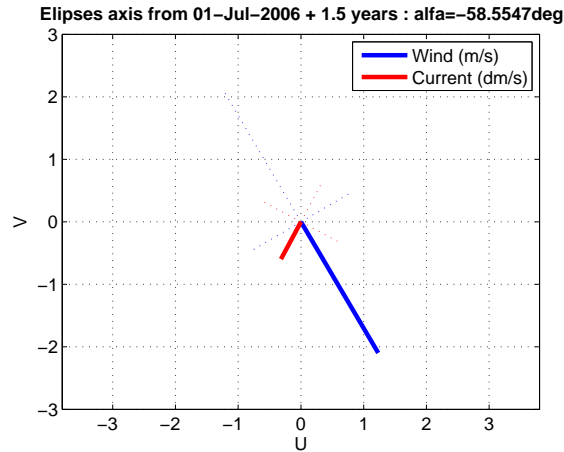


Figure 9. Principal axis analysis – Values correspond to variance and alfa is the angle between the two full lines. (Monterey station.)

The table shows values for each term:

Principal axis for W/C: from 01-Jul-2006 + 1.5 years

	theta	Maj.	min.
wind	-30.4301	4.8623	1.9311
current	28.1246	0.13539	0.13232

Table 4. Principal axis analysis. – Values correspond to magnitudes and angle between the major axis and north. (Monterey station.)

The results of all the time series show that magnitudes of the variance keep within the same order. The angles vary more, getting dispersed as we reduce the time series length. The average angle between the two major variance directions is around 50 degrees in the longer time-series as shown in Table 5.

Examples of results from the different stations in different periods

Station	Period	Angle between major axis (°)
MRY	01JUL06 .. 31DEC07	-59
HMB	01JUL06 .. 23NOV06	-14
	20FEB07 .. 12JUL07	-8
	04SEP07 .. 31DEC07	-10
SFR	29NOV06 .. 07JAN07	-2
	01MAR07 .. 26MAY07	-15
	06SEP07 .. 31DEC07	-19
M0	11OCT06 .. 28MAR07	-39
	29MAR07 .. 25JUN07	+21
	25JUN07 .. 31DEC07	+25
M1	16NOV06 .. 05JAN07	-43
	24APR07 .. 24JUN07	+1
	25JUN07 .. 30AUG07	-6

Table 5. Principal axis analysis. – Space and time variability (wind – current.)

Despite the tendency for the longer time series, the high variability does not allow a good estimation of a typical angle between wind and current, demonstrating that it may be more a function of time and place.

## 2. Complex Correlation (Kundu, 1975)

Complex correlation gives a measure of correlation between two complex time series. The magnitude of the result shifts between 0 and 1, 1 being if the signal is the same. The average phase angle gives an idea of the physical angle between the two phenomena. Results for the Monterey station are plotted on Figure 10, and results for all stations are tabulated in Table 6.

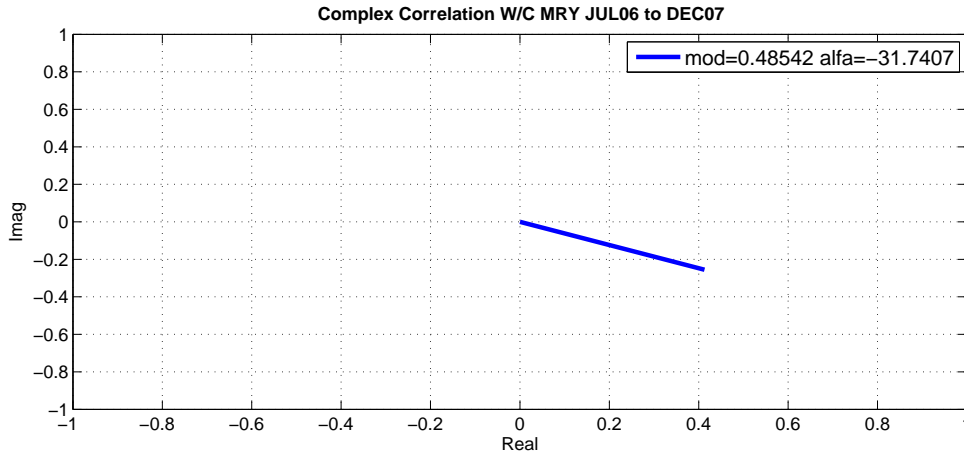


Figure 10. Complex correlation – Modulus is a measure of correlation and alpha is the physical angle. (Monterey station.)

The magnitudes vary from 0.2 to 0.7. The angles tend to remain on the second quadrant around 35 degrees, gaining variance with the reducing of the length of the time series. These results mean that they are correlated, and there is in average 35 degrees between the directions of the two. This is expected because the angle is supposed to increase in time, until Ekman’s 45 degrees. The results for M0 buoy present the highest variability but also the smaller correlation, probably due to the variability of the winds and currents inside the Bay. An attempt was made to verify if the correlation would increase when lagging the Current time series, but it decreased, pointing to zero lag.

Examples of results from the different stations in different periods

Station	Period	Magnitude	Angle (°)
MRY	01JUL06 .. 31DEC07	0.49	-32
HMB	01JUL06 .. 23NOV06	0.31	-56
	20FEB07 .. 12JUL07	0.66	-47
	04SEP07 .. 31DEC07	0.48	-56
SFR	29NOV06 .. 07JAN07	0.66	-1
	01MAR07 .. 26MAY07	0.81	-16
	06SEP07 .. 31DEC07	0.62	-23

Station	Period	Magnitude	Angle (°)
M0	11OCT06 .. 28MAR07	0.34	-26
	29MAR07 .. 25JUN07	0.27	-83
	25JUN07 .. 31DEC07	0.17	-45
M1	16NOV06 .. 05JAN07	0.5	-34
	24APR07 .. 24JUN07	0.67	-17
	25JUN07 .. 30AUG07	0.69	-13

Table 6. Complex correlation. – Space and time variability.

### 3. Scatter Comparison

Scatter plots give an idea of correlation and permit a mathematical best-fit expression (e.g., Figure 11, Figure 12, Figure 13). A perfect correlation happens when all the pairs of values (points) of the two time series design a mathematical expression. This will allow elaboration of the best transfer function relation in terms of magnitude. The one presented here considers the full energy spectrum, and the best fit is accomplished with a quadratic expression.

This analysis can also be done by frequency bands if the choice is to transfer by frequency. As we will see later, the degree of added complexity for such an approach will not increase significantly the results of the first one.

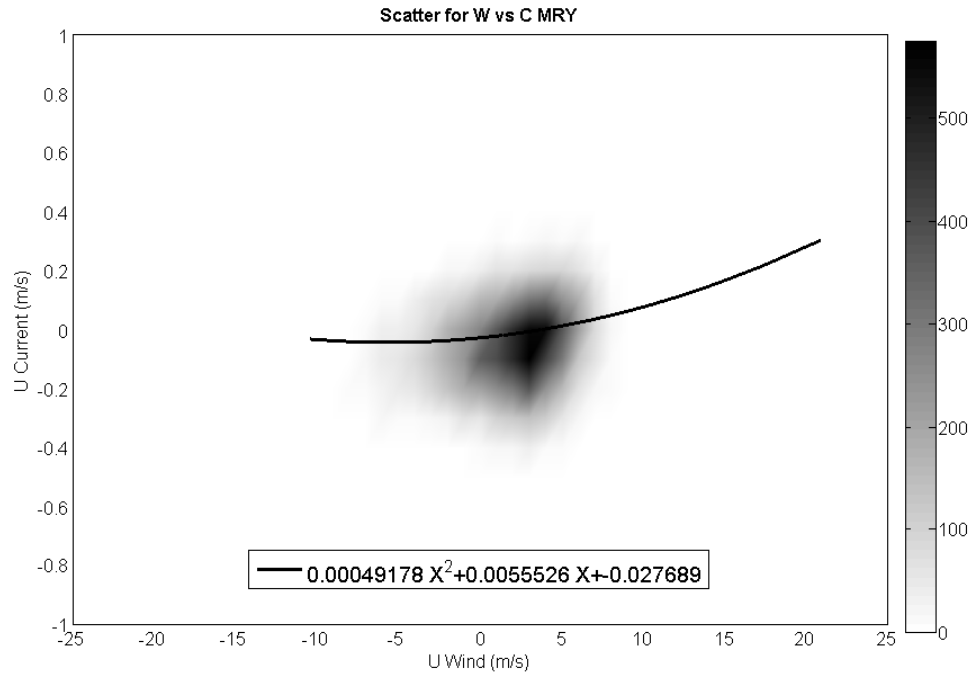


Figure 11. Scattering diagram for U and best fit expression. (Monterey station, Jul 06 to Dec 07.)

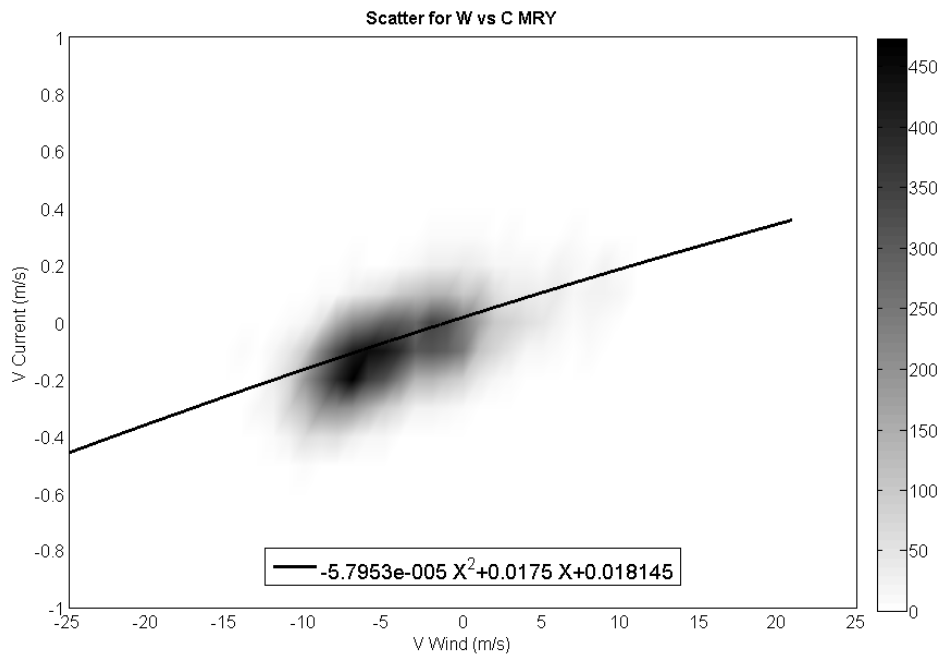


Figure 12. Scattering diagram for V and best fit expression. (Monterey station, Jul 06 to Dec 07.)

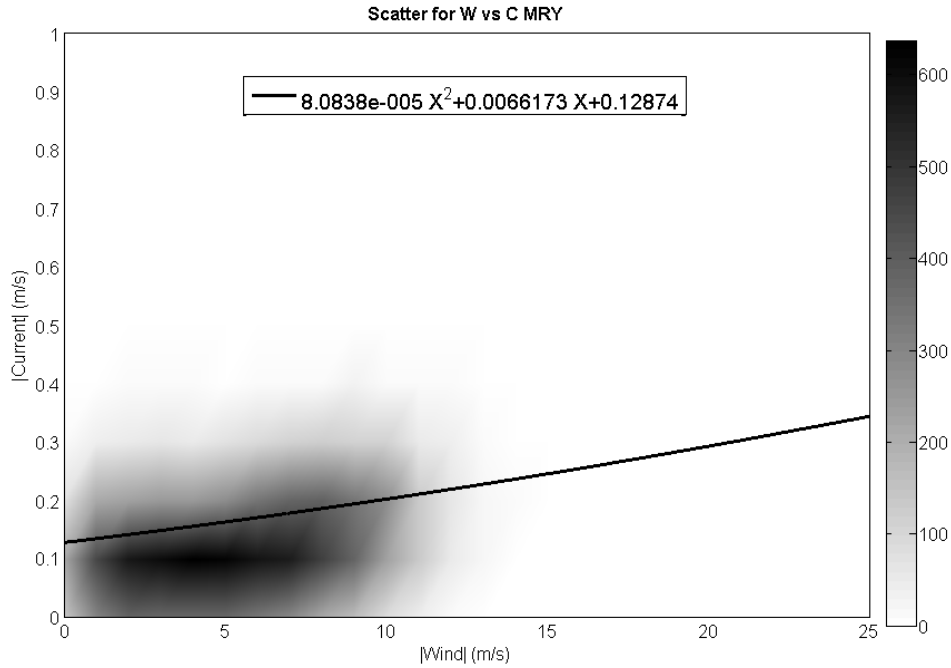


Figure 13. Scattering diagram for Modulus and best fit expression. (Monterey station, Jul 06 to Dec 07.)

After applying it to all the series, including the rotated ones, the best proxy for the typical expression relating near surface wind to surface current, in terms of magnitude of the vector, is:

$$C = 0.018U_5 + 0.03 \quad (8)$$

where  $C$  is the surface current in m/s and  $U_5$  is the wind at 5 m height, also in m/s.

The quadratic term shown on the figures is always positive and negligible, with some exceptions in the modulus when it goes negative. The results presented here are restricted to the linear terms in the fit. Those values multiplying by  $U_5$  vary plus or minus 0.02. But, overall, the results show surface current magnitudes are very close to 2% of the wind speed magnitudes (Table 7). The choice of 0.018 is supported by the error analysis and tuning done in the forecast section. The last constant varies plus or minus 0.05. This variation tends to be smaller in winter and fall and in the fits based on longer time series. This expression will be tuned in the predicting algorithm in Section III.

Examples of results from the different stations in different periods

Station	Period	U	V	Modulus
MRY	01JUL06 .. 31DEC07	0.006X-0.028	0.018X+0.018	0.007X+0.128
HMB	01JUL06 .. 23NOV06	0.001X-0.063	0.021X+0.096	-0.016X+0.217
	20FEB07 .. 12JUL07	0.000X-0.047	0.017X-0.068	0.001X+0.178
	04SEP07 .. 31DEC07	-0.006X-0.045	0.018X-0.013	0.007X+0.167
SFR	29NOV06 .. 07JAN07	0.013X-0.031	0.022X+0.037	-0.016X+0.162
	01MAR07 .. 26MAY07	0.013X+0.000	0.018X-0.033	0.006X+0.175
	06SEP07 .. 31DEC07	0.007X-0.012	0.023X+0.004	0.013X+0.106
M0	11OCT06 .. 28MAR07	0.005X-0.014	0.007X+0.001	0.001X+0.099
	29MAR07 .. 25JUN07	0.001X-0.089	0.004X+0.032	0.006X+0.114
	25JUN07 .. 31DEC07	0.004X-0.039	0.006X+0.017	0.006X+0.104
M1	16NOV06 .. 05JAN07	0.008X-0.039	0.016X+0.041	0.007X+0.111
	24APR07 .. 24JUN07	-0.009X+0.025	0.008X-0.028	-0.005X+0.149
	25JUN07 .. 30AUG07	0.005X+0.001	0.010X+0.007	-0.015X+0.177

Table 7. Best fit expression. – Space and time variability.

#### 4. Auto Correlation (McMahan and Wyland, NPS Lab Software, 2007)

Autocorrelation of a given time series allows for a better understanding of the time scales involved. Each oscillation represents the time scale of an active agent. Examples are shown for wind and current in Figure 14 and Figure 15, respectively.

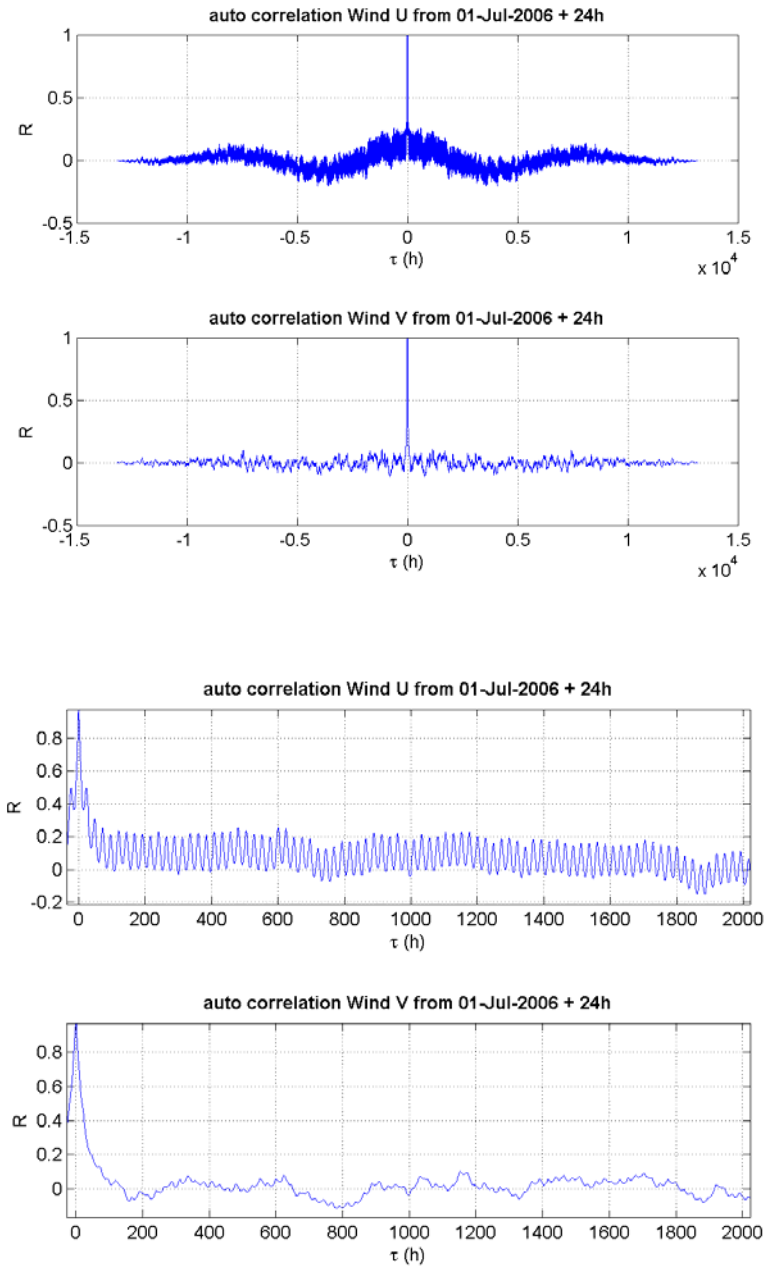


Figure 14. Autocorrelation for Wind – The bottom is a zoom of the first positive 2000h ~ 3 Months. Daily, synoptic and monthly oscillations are present. (Monterey station, Jul 06 to Dec 07.)

Concerning the wind, the influence of the sea breeze is easily seen on the U component in the small oscillations of 24 h. On both, we can also see an oscillation around the 6 days (synoptic scale). In U, monthly and a seasonal oscillations are also present.

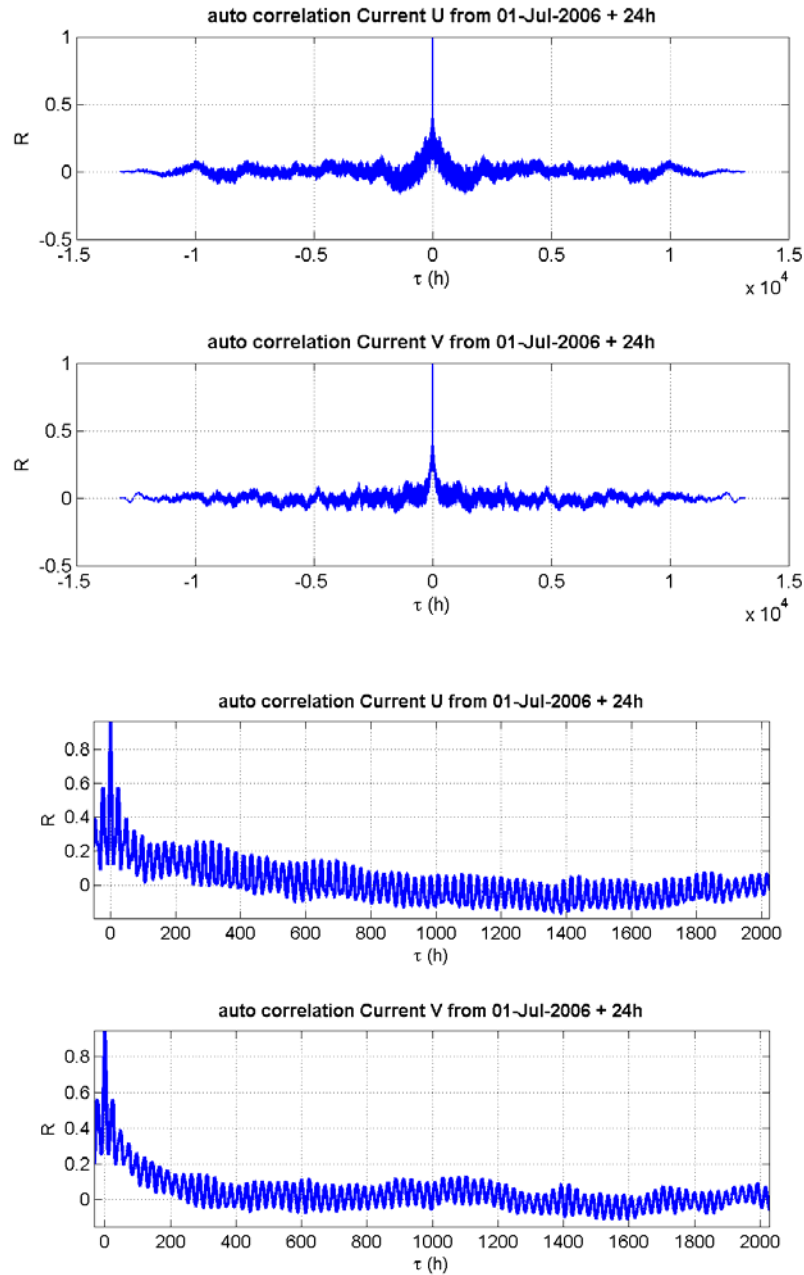


Figure 15. Autocorrelation for Current – The bottom is a zoom of the first positive 2000h ~ 3 Months. Daily, synoptic and monthly oscillations are present. (Monterey station, Jul 06 to Dec 07.)

For the current, daily, synoptic and monthly oscillations are noticed as well. The tidal influence can be easily seen from the difference between Figure 15 (simple current measurement) and Figure 16 (after tide removal). Daily, synoptic and monthly oscillations are present, but the daily one is much less energetic. All the daily oscillations tend to be bigger in the summer. There is no important change looking between stations, except in the magnitude of the oscillations.

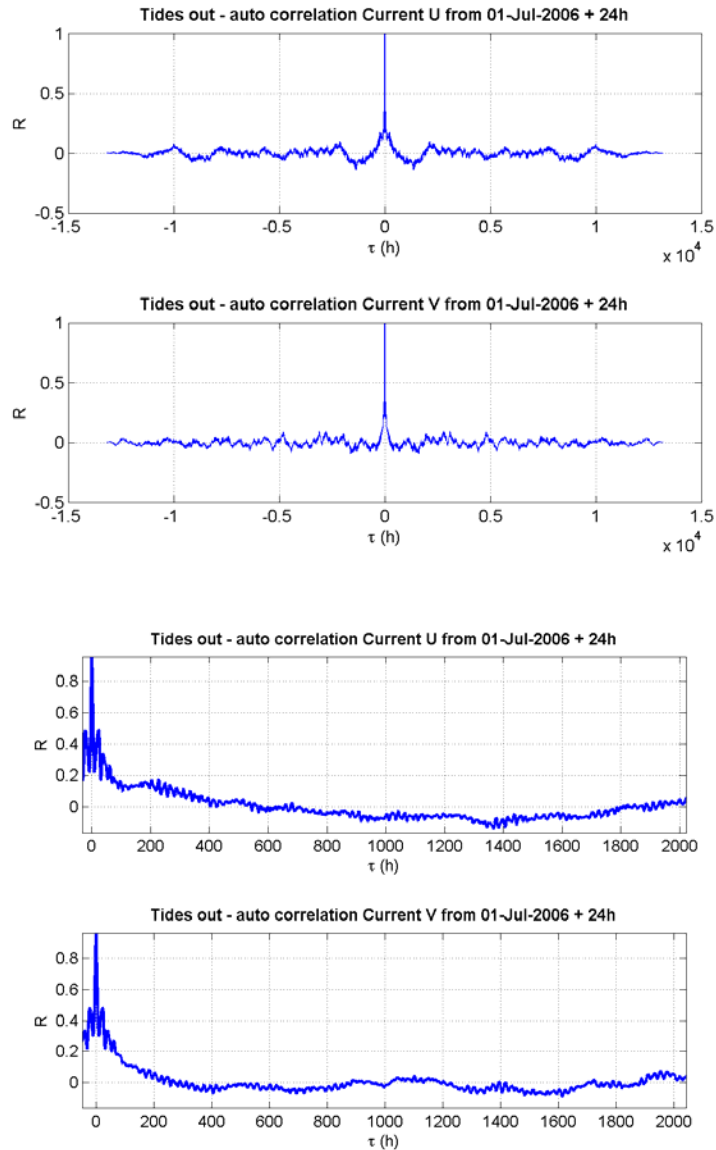


Figure 16. Autocorrelation for Current with tides removed – The bottom is a zoom of the first positive 2000h ~ 3 Months. Daily, synoptic and monthly oscillations are present. (Monterey station, Jul 06 to Dec 07.)

## 5. Power Spectra and Straight Coherence

The power spectra of wind and current give the distribution of energy versus frequency (Figures 17 and 18). Based on this, coherence gives the significance of the relation of the signals for each frequency and the phase difference between them (Figure 19).

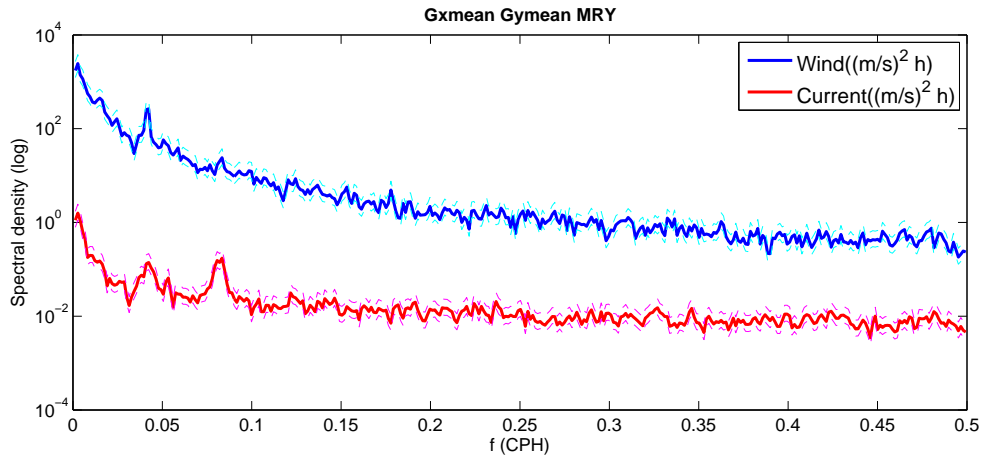


Figure 17. Power spectra of Wind and Current – Dashed at 95% confidence. (Monterey station, Jul 06 to Dec 07.)

The peaks for the daily and 12h periods are easily spotted in both wind and current. Winds are especially energetic in the sea breeze period while the currents show almost equivalence on both, maybe because of the previously mentioned wind and tide correlations. After the tide signal removal attempt, both current peaks are slightly smaller, representing less energy. When removing tides by best fit of frequencies, we are removing also part of the wind influence which shares those same frequencies – the sea breeze.

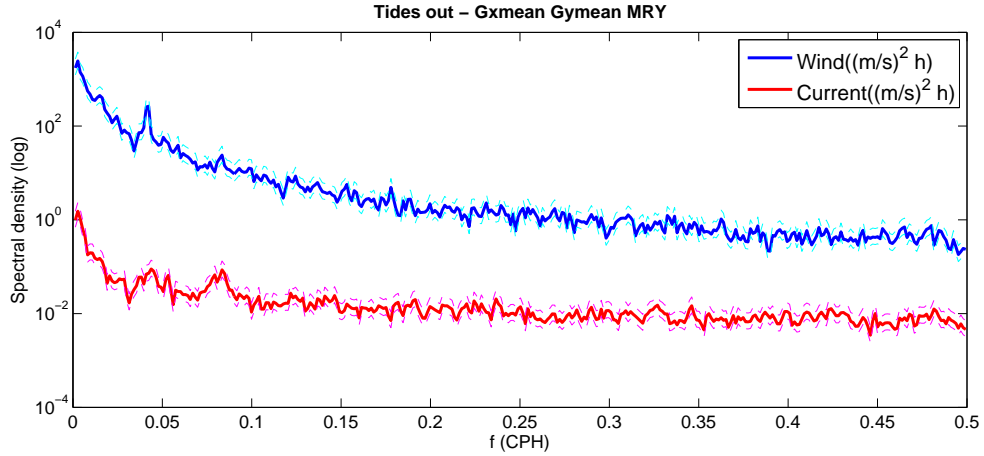


Figure 18. Power spectra of Wind and Current with tides removed – Dashed at 95% confidence (Monterey station, Jul 06 to Dec 07.)

Adding the variances both with and without tides, we notice the slight decrease in energy that is removed. The results are summarized in Table 8.

Difference of with and without tides

wind variance	19.5694
tides in - current variance	0.016719
tides out - current variance	0.015593

Table 8. Added variances ~ energy. (Monterey station.)

These series are significantly coherent for periods longer than a day. During this interval, the phase augments from near zero to around 60°. In the shorter time series the coherence is consistent only after 40 h, and the phase tends not to exceed 50°. When done by components (u and v) it is coherent after approximately 12 h.

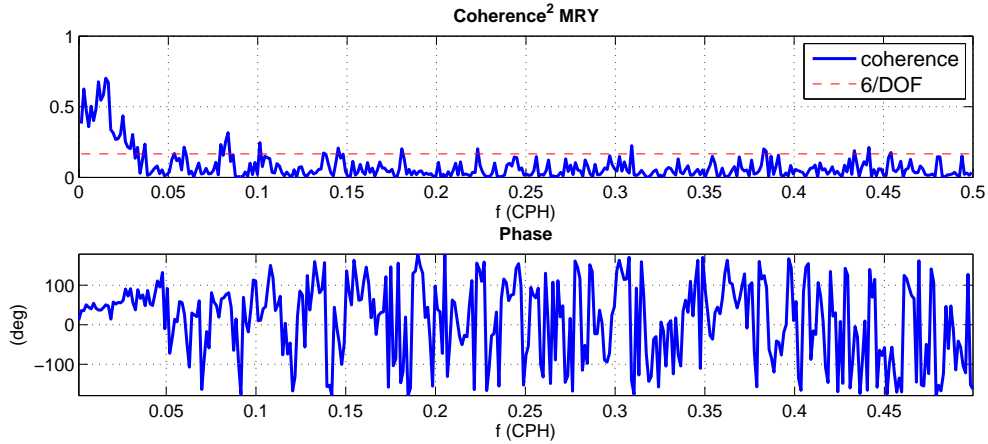


Figure 19. Coherence and Phase between wind and current – Dashed at 95% confidence. (Monterey station, Jul 06 to Dec 07.)

## 6. Rotary Spectra (Gonnella, 1972 and Mooers, 1972, Bahr, 2007 Software)

Rotary spectra subdivides a signal into two rotating components, one clockwise and the other counter-clockwise. This allows one to analyze the coupling of two signals in terms of their rotating behavior, giving independence from the axis choice. Results for wind and current for the Monterey station are shown in Figure 20 and Figure 21, respectively.

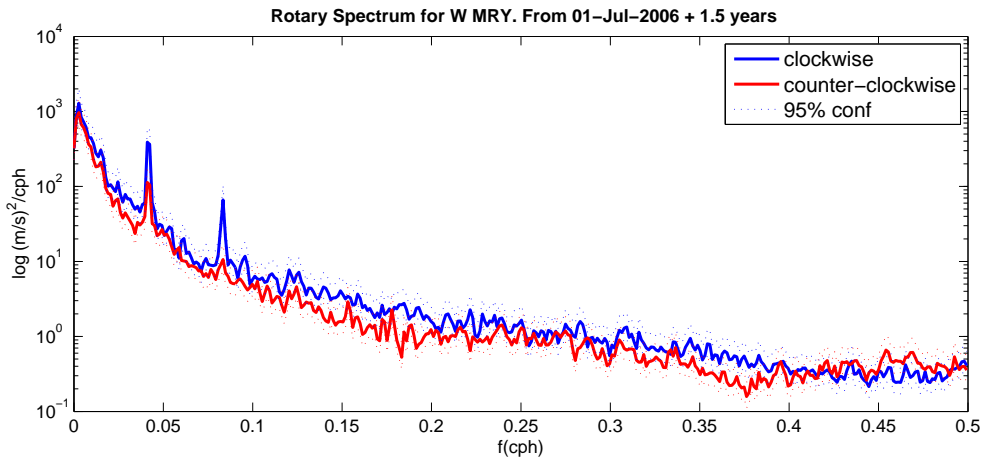


Figure 20. Rotary components for wind – Notice the two peaks for 12 and 24h. (Monterey station, Jul 06 to Dec 07.)

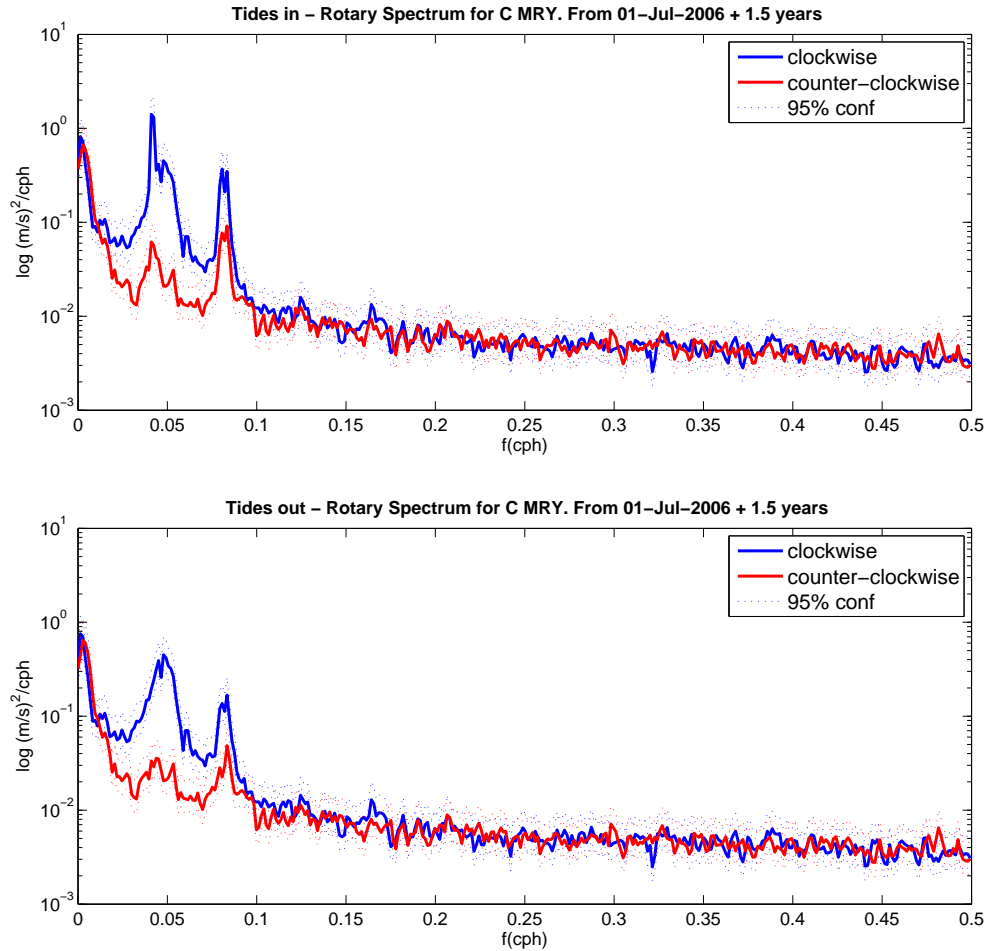


Figure 21. Rotary components for current, tides in and out – Notice a small decrease in energy. (Monterey station, Jul 06 to Dec 07.)

The two diurnal and semi-diurnal peaks are distinct in both wind and current, reflecting the importance of such frequencies. Notice that the clockwise component is bigger, the peaks being more similar to the 24h point in the wind and the 12h in the current. The current peaks are only a little smaller after the tides’ removal.

The “rotary coefficient” is a measure of the purity of the signal in terms of rotation: a fully rotating signal is 1, a non-rotating is 0. The rotary coefficient for the wind and current records at the Monterey station are shown in Figure 22 and Figure 23, respectively. Distinctively, for periods under 12h, the current is more rotational than the wind, which only shows two small peaks in the frequencies of interest.

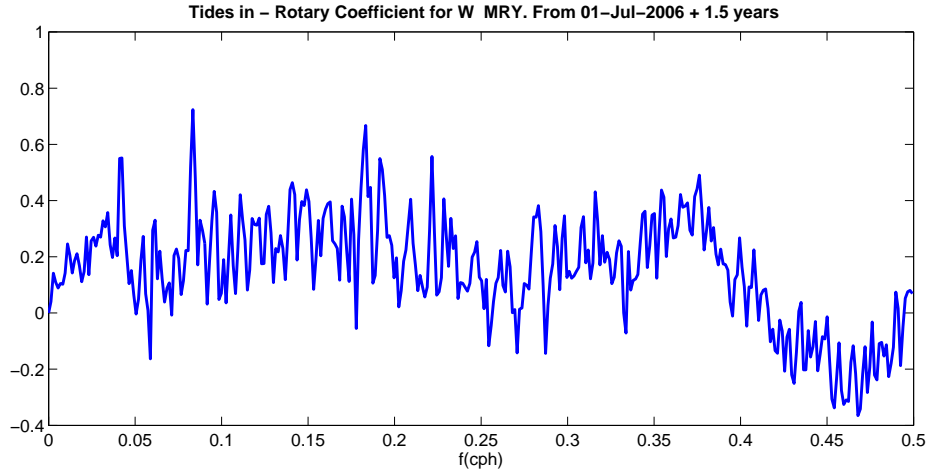


Figure 22. Rotary coefficient for Wind – A fully rotational movement would be valued 1. (Monterey station, Jul 06 to Dec 07.)

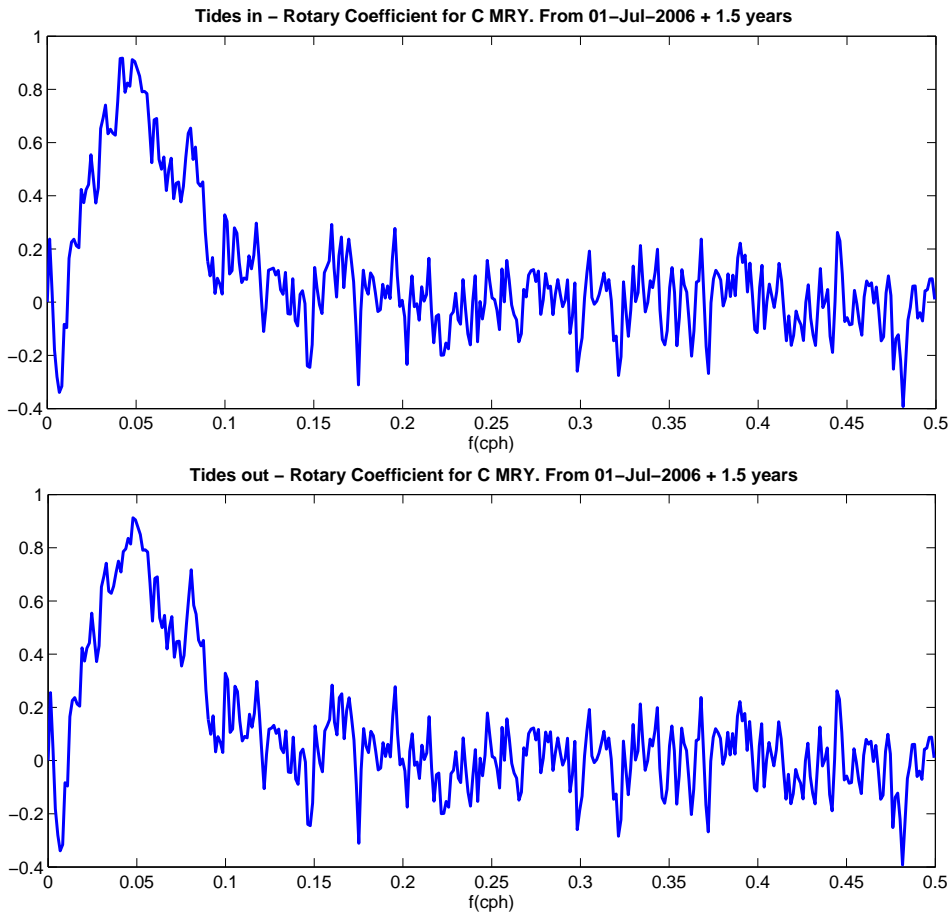


Figure 23. Rotary coefficient for Current, tides in and out. (Monterey station, Jul 06 to Dec 07.)

**7. Vector Cross Spectral Analysis (Mooers, 1972 and McNally et al, 1989, After Jessen and Bahr, 2007 software)**

Vector cross spectral analysis is a tool to check the coherence between two rotary signals. Plugging in wind and current, the coherence results for the Monterey station are shown in Figure 24.

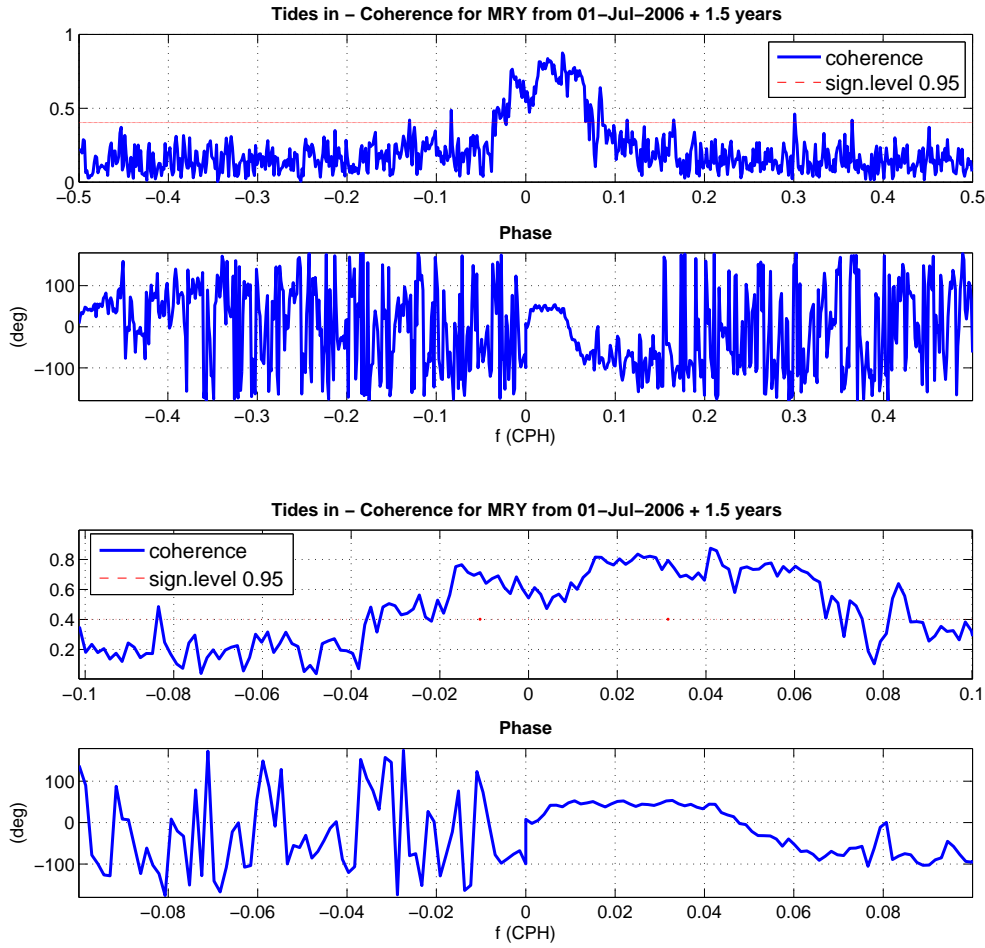


Figure 24. Complex Coherence and Phase – Lower image is a zoom of the coherent part. (Monterey station, Jul 06 to Dec 07.)

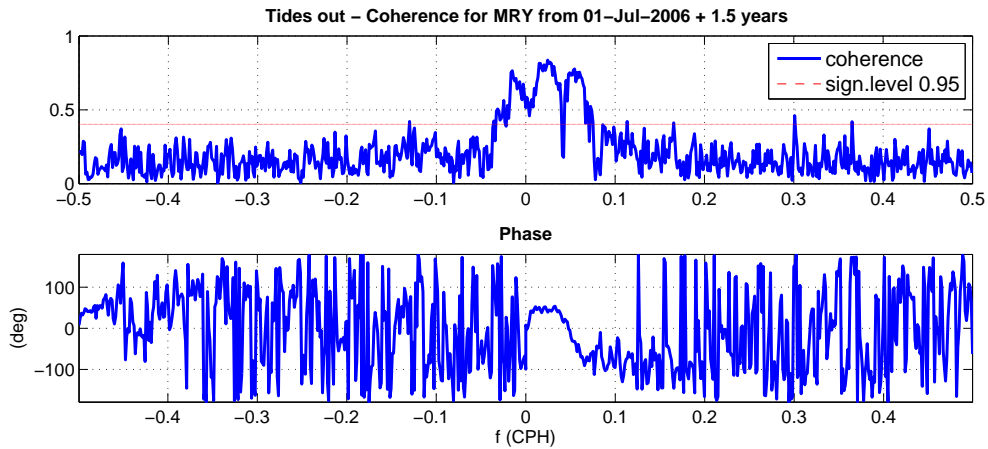
The application of this method allows one to calculate, besides the coherence, the angular shift in time. Table 9 shows the average results for the coherent-positive part.

### Complex Coherence results

Time (h)	Angle (°)
20	30~35
30	40~45
60	45~60

Table 9. Wind and Current shifting of angles in time. (Averages for all the stations and periods.)

After 17h almost all the series are coherent and have a much slower variation. For periods between 0 and 17h the results were inconclusive. This treatment is done also to the velocity square, to search for a difference between pure wind velocity and wind stress (function of the velocity square). No significant difference was found between the coherence results for wind or wind stress. For the de-tided series, the relation keeps its results except during the 24 and 12h periods, where very narrow positive and negative peaks appear (Figure 25), probably a result of energy removal in those frequencies.



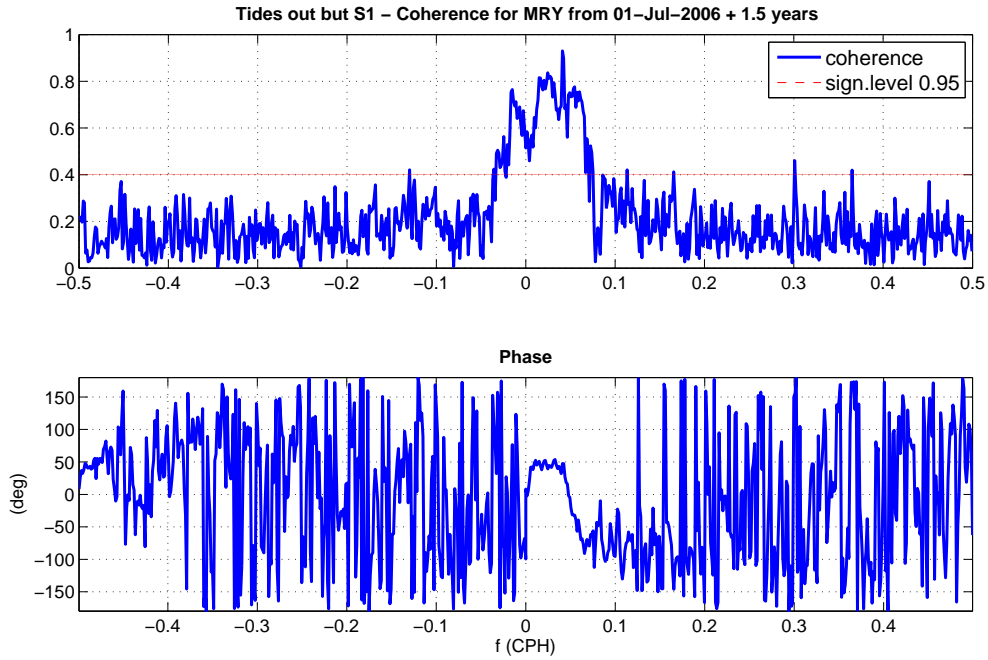


Figure 25. Complex coherence and Phase, tide removed – Top, all constituents. Bottom, all constituents removed but S1. (Monterey station, Jul 06 to Dec 07.)

Comparing results for other stations (not shown), the M0 buoy is only coherent after 24h at a 50° phase. The same can be said for M1 in the summer.

The empirical approach gave us estimation of the interaction between the wind and the surface current in its magnitudes and phase shifts. This allows building a transfer function that will later be used to forecast the current, having the forecasted winds in consideration of various factors.

#### D. THEORETICAL APPROACH

In this approach, theory is used to compare with the empirical results. Calculations are made using Ekman's works theory, and a function is created considering:

$$\tau_{0x} = \rho_a C_D U_{10}^2 \cdot \quad (9)$$

And at the same time

$$\tau_x = \rho_a A_v \frac{\partial u}{\partial z}. \quad (10)$$

So, adding the two and rearranging,

$$\partial u = \frac{\rho_a C_D}{\rho_0 A_v} \cdot \partial z \cdot U_{10}^2. \quad (11)$$

The magnitude of  $U_{10}$  is taken to be approximate of  $U_5$ , for it is the top part of the exponential wind growth in height; the Yelland and Taylor, 1995 drag coefficient is used as function of the wind speed.

## E. COMPARISON

Having the empirical and the theoretical result transfer functions, and using  $U_{10} = 10$  m/s we obtain:

1. From the results of the study in equation (8),
 

**du=0.21 m/s.**
2. From the theoretical result of (11),
  - a. Ekman depth = 50m and  $A_v=0.01$  m<sup>2</sup>/s      du=0.68 m/s;
  - b. Ekman depth = 10m and  $A_v=0.01$  m<sup>2</sup>/s      **du=0.27 m/s;**
  - c. Ekman depth = 50m and  $A_v=0.3$  m<sup>2</sup>/s      du=0.02 m/s;
  - d. Ekman depth = 10m and  $A_v=0.3$  m<sup>2</sup>/s      du=0.01 m/s.

This means that the theoretical result is highly dependent on a good estimate of eddy viscosity, and that using a typical value ( $A_v \sim 0.01$ ), Ekman depth must be much shallower. Using typical values, Ekman theory overestimates the change in the surface current velocity.

## F. CONCLUSIONS

Having studied the wind / surface current interaction in different perspectives, times and spaces, the relationship found can be described as follows.

## 1. Transfer Function

### a. *Magnitude*

The surface current generated is around 2% of the wind speed.

### b. *Angle*

The angle measurement increases in an unknown way until around 17h. From then on, the angles vary from 35° to 60°, according to Table 9.

## 2. Notes

Despite these results, the scatter plots show a large dispersion, which means that there is a high variability.

The unknown growth until 17h includes wind wave interaction. It includes also components of transfer from 0 to 35° of some magnitude.

In this study, rotating the axis to biggest variance or long-shore, cross-shore, does not bring any significant change, probably because of the meridional characteristic of the Californian coast. Nevertheless, when using both wind and current axis to their respective biggest variances, the component minor wind axis versus minor current axis does tend to zero.

The tidal removal does not bring major changes to the transfer function as a bulk. If transferred by frequency, care has to be taken especially in the inertial periods and its subdivisions.

### **III. THE FORECAST**

#### **A. FORECAST WITH CODAR**

Forecasting with a remote sensing means like CODAR has the enormous advantages of independence and timing--independence because it does not rely on any other system to operate, and timing because it is updated every hour. This is more than enough to get good estimates for the surface currents variability, making data available when needed. Nevertheless, relying only on previous surface currents readings from our own system has its dangers and limitations. As will be shown, coupling our readings with those of other systems yields more reliable and accurate results.

##### **1. Reliability of a Forecast**

CODAR has proved to be a very reliable system, so far. Nevertheless, its results may be misleading. Once it uses electromagnetic radiation to operate, it is subject to all its difficulties and laws, as described by the following examples.

- If an object with electromagnetic potential and length comparable to the transmitted wavelength (approximately 10m) goes near the antennas, the reception pattern changes, leading to deviation in the result;
- The presence of a moving target, such as a ship, may introduce an error due to strong backscatter;
- A change in the background radio frequency properties will influence the signal also.

These and other problems have been addressed several times, and are adequately explored in several works (some of which can be found on <http://www.codaros.com>). The use of a second system allows us to detect possible malfunctions by comparison, and gives a different set of solutions as backup. This is always preferable.

##### **2. Accuracy of a Forecast**

The accuracy of the system is dependent on the errors of CODAR (8 to 18 cm/s, from Wright, 2008), plus the ones associated with the estimation of the next 24h behavior (the assumptions and the errors of the systems we are building our prognostic on), plus

the error of what we cannot or do not predict. If we introduce to our algorithm a good description of the future conditions and have good relation functions, we will obtain a more realistic result.

So, coupling with other systems, as upload or download, is advantageous. We can obtain data from tides, winds, drifters, current meters, and models--and can assimilate our results back into the models.

## **B. PREVIOUS ATTEMPTS**

The previous attempt model is described in I B. The results have been generally accurate for persistent weather conditions, but tend to get worse with changing weather conditions.

### **1. Problems**

The model was based only in tidal and persistence analysis. Once any of the conditions--wind, waves, or any other parameter--changes, the persistence does not follow. In weather, significant changes can happen in any 24h period.

### **2. Results**

As pointed in I.B., there is still lack of confidence in this model any time there is a significant change in the weather (namely in current velocity and possibly wind). A summary of results for the previous tidal model applied to the region offshore San Francisco is shown in Figure 26. Here a pixel grid of pseudo drifters release points was used to create predicted trajectories for 24h, which was repeated each hour for the period August 2006 through July 2007. The plot shows the rms spatial difference between the end points of the predicted trajectories compared with the observed trajectories one day after. The negative correlation with number of drifters (lower panel) reflects the fact that higher speed conditions result in more pseudo drifters, leaving the sampling grid within a 24h period. The direct effect of wind speed on the spatial accuracy of the predicted trajectories is less clear. Nonetheless, wind (specifically wind changes) is hypothesized to explain some error in forecast currents.

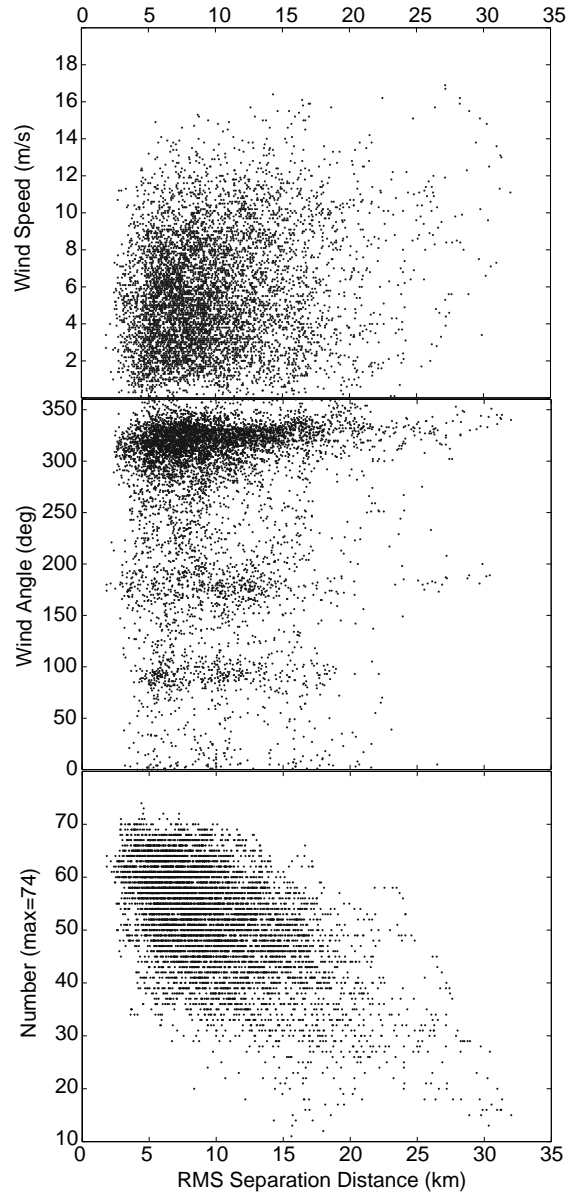


Figure 26. Results for RMS compared with wind and number of pseudo drifters – RMS for 24h. The number of pseudo drifters present may be used as a proxy for current speed. (Image from Garfield et al., 2007.)

### C. THE INTRODUCTION OF WIND

One attempt to reduce forecast error is the introduction of wind influence. A study of the wind surface / current interaction was made for this thesis and is described in Section II. The objective was to build a transfer function that allows us to plug in the wind driven current into the forecast. Several approaches were considered: transfer by

frequency, transfer by different division of spatial and time components, transfer as a vector, transfer with tide analysis, and transfer based on persistence. The approaches that seemed to be more efficient for practical purposes (accuracy versus simplicity) narrowed to only one wind/current transfer function and transfer as a vector. Transfer by frequency was not chosen because of the relatively small magnitude of the end results. Tide removal and simple persistence conditions would have yielded similar results. The models tested were based on the diagram in Figure 27, regardless whether or not tides were removed.

The winds had different methodologies applied also in terms of what time slice constituted future for computing wind differences and whether or not to use wind difference compared with removing and then reintroducing the full wind-driven current. The results were practically the same. In this hindcast study, forecast wind is taken from the actual readings, simulating a zero error wind forecast. The methodology tested here can, however, be immediately transferred to winds forecasted by an atmospheric model such as the Navy's COAMPS model.

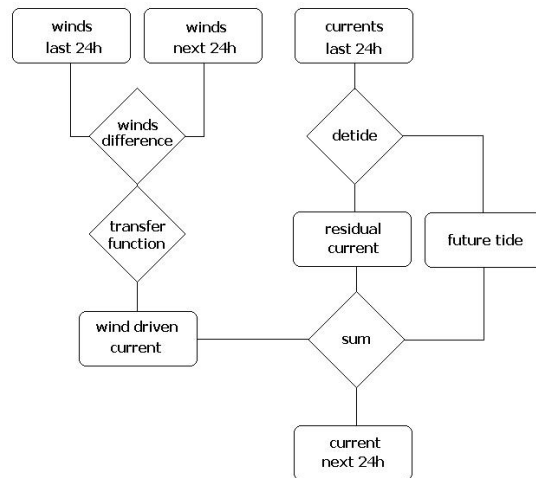


Figure 27. Basic flow chart diagram of the forecast procedure – Several adaptations were attempted.

### 1. With Tides Treatment

This attempt corresponds exactly to the previous diagram. The best results were obtained using the following procedure.

We are at t=0 and we want the next 24h surface currents forecast, so we

- Take the last 24h current readings;
- Remove the tides by “t\_tide” using all the previous month’s currents to the best fit. Conducting the detiding with using one month of data or just three days of data both returned good results as shown in Table 10.

Detidal associated errors

RMS (m/s)	3 Days	1 Month
U	0.1087	0.1073
V	0.1027	0.1145
modulus	0.1515	0.1593

Table 10. Detidal errors with 3 days and 1 Month data – The calculation of the Root Mean Square error will be discussed in III. E. (Monterey Station.)

- Forecast the tide for the next 24h using “t\_predic” and the structure of constituents that resulted from the detiding;
- Low pass filter the residual current to 18h;
- Average the residual current;
- Take the last 24h wind readings;
- For each hour in the future h, get the forecast wind from that hour until t=0 and the wind readings before that until h-24;
- Low pass filter both to 18h;
- Do the average for each;
- Take the difference of the winds;
- Use the transfer function to get the current associated with the wind difference;
- Sum the residual current, the tide and the wind current.

Figure 28 is an example of the obtained result, in a day where a major wind change took place and the wind influence is noted. The resolution is hourly.

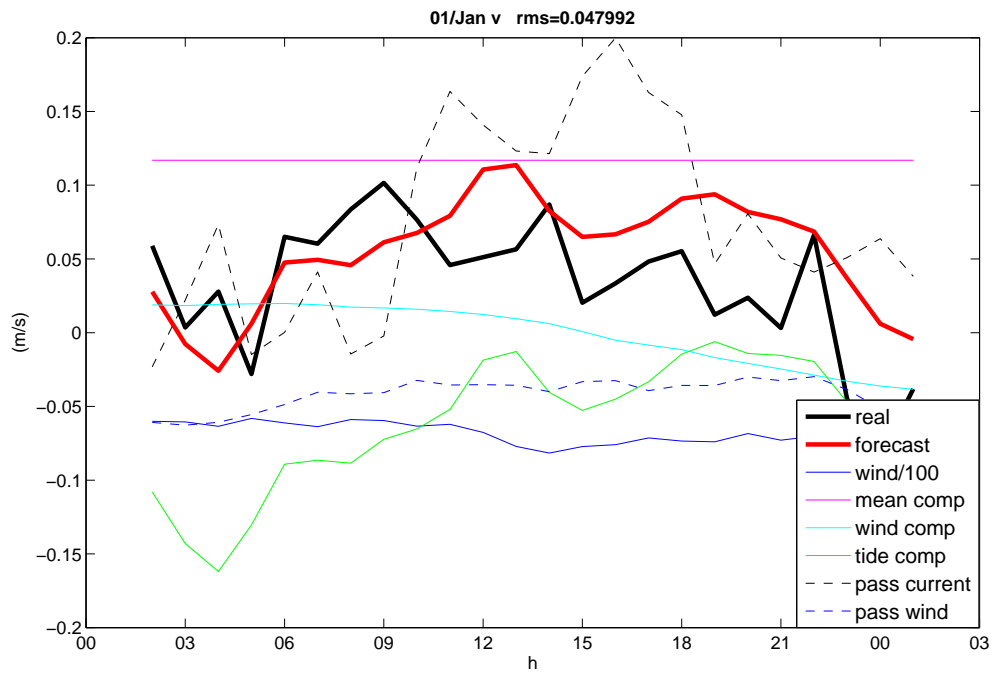
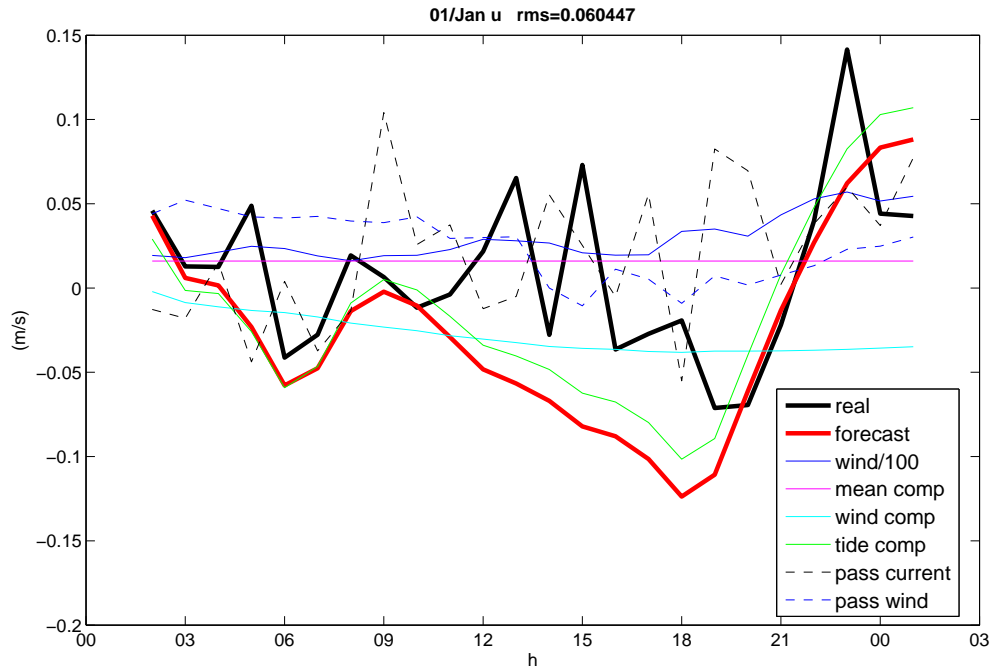


Figure 28. One day forecast with tide treatment – The wind changing its influence. (Monterey Station.)

## 2. With Persistence

The procedure sequence is the same as the above but with the major difference of not removing the tidal influence. This method uses the last 24h current readings as the current for the next 24, summed with the wind difference driven current. Example results using the persistence model are given in Figure 29.

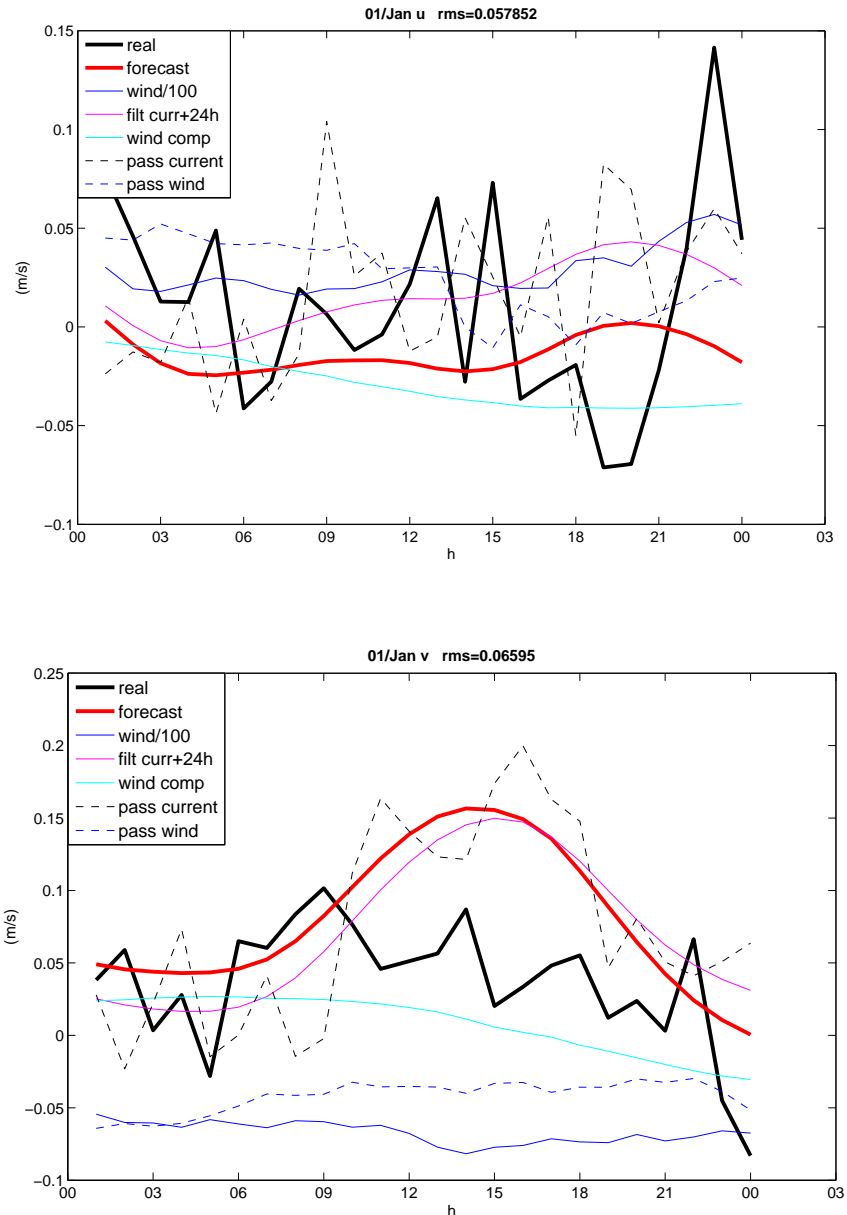


Figure 29. One day forecast with persistence – The wind changing its influence. (Monterey station.)

## D. TUNING

The wind interval to account for the difference between forecast and real is chosen after several different runs bases on shifting the future wind interval for several periods forward. The one with least error is the one designated, where the wind interval ends at  $t_p$  (Figure 30). Several values around the transfer function were also attempted. The best results are obtained with a 50° clockwise rotation, and with a magnitude

$$C_{wind} = 0.018U_5 + 0.018. \quad (12)$$

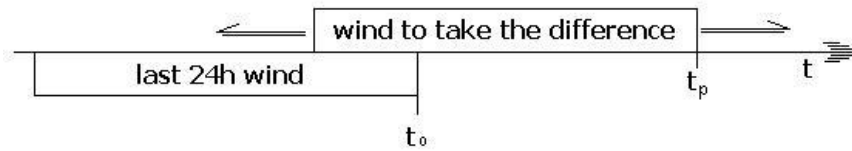


Figure 30. The difference between winds – Several positions of the future wind interval were attempted for a given time of prediction ( $t_p$ ).

## E. COMPARISON

RMS is calculated on a daily basis with and without introducing the wind . RMS is based on the difference between our calculated surface current for each hour and the actual CODAR reading at that time. This means that we are considering CODAR as “true.” We must take into account the CODAR intrinsic variability when analyzing results. The end RMS result for each component u and v is:

$$RMS_{component} = \frac{\sqrt{\sum_1^N (reading - forecast)^2}}{N - 1} \quad (13)$$

with the total

$$RMS_{total} = \sqrt{RMS_U^2 + RMS_V^2} . \quad (14)$$

The results are given in Table 11, considering a normal distribution.

	(m/s)	average	Variance	Standard deviation	95% conf (+/-)	99% conf (+/-)
Tide removal	RMS With wind	0.1593	0.0022	0.0471	0.0923	0.1213
	RMS No wind	0.1667	0.0028	0.0529	0.1036	0.1363
Persistence	RMS With wind	0.1427	0.0023	0.0482	0.0945	0.1242
	RMS No wind	0.1495	0.0028	0.0528	0.1035	0.1360

Table 11. Root Mean Square comparison – Average daily values. (Monterey station, Jul 06 to Dec 07.)

The statistical results for the 18-month study period show that the wind influence is one order of magnitude inferior to the total error. Use of persistence or tide treatment yields practically similar results, with simple persistence of today’s observed low pass-filtered currents giving slightly better results.

Looking at other station results, station M0 gets the least error results, followed by M1, probably due to the repetitive nature of the flow in that position, or perhaps because it is more protected from unaccounted variations. Results distributed by station are shown in Figure 31. There is a visible relation between error and stations, showing that the error causes are probably associated with the position and its typical patterns of wind, currents, the radar station itself, and other features. This will be studied more closely in Section III.F. Interestingly, the distributed results show clear, positive correlation between forecast error and the mean station current speed or current variability, which is consistent with the previous findings of Garfield et al., 2007.

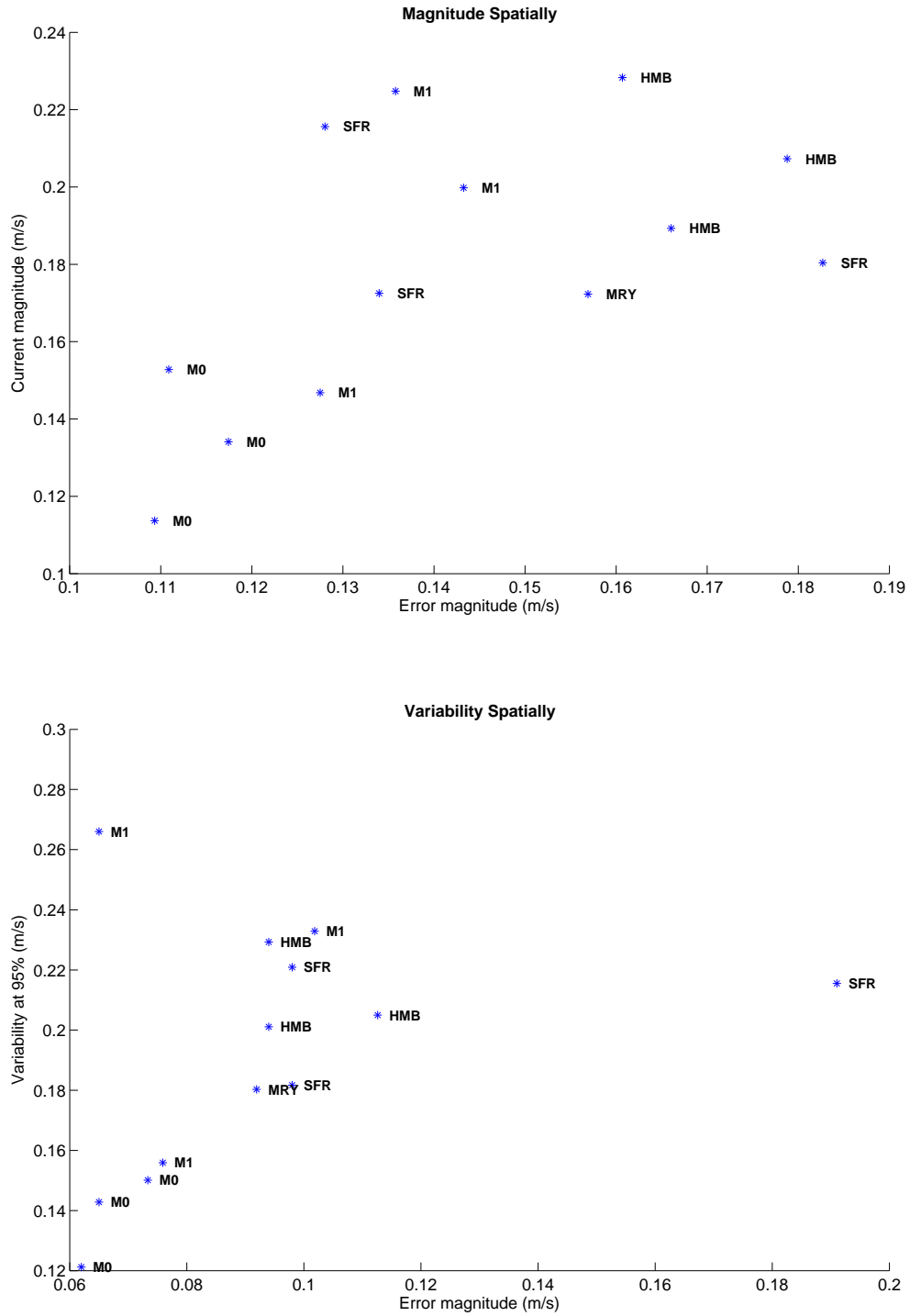


Figure 31. Relation of RMS error and the stations – Top is magnitude of the current vs. error. Bottom is variability vs. error. Based on the tide plus mean with transfer function model forecasts.

Seasonality does not seem to play a major role, but the small quantity of data does not allow a definitive conclusion. The four-season results for the Monterey station are shown in Figure 32.

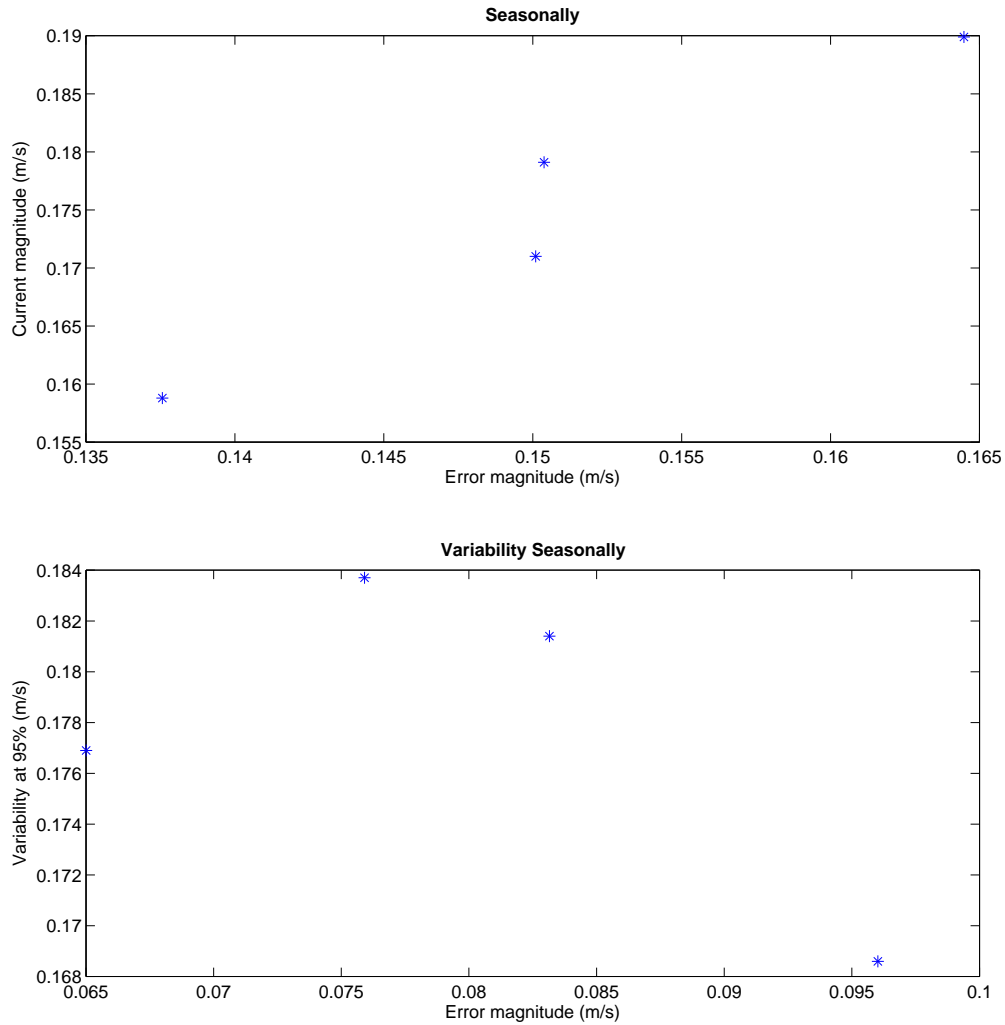


Figure 32. Relation of RMS error and seasons – Top is magnitude of the current vs. error. Bottom is variability vs. error. (For Monterey station, based on the tide plus mean wind transfer function forecasts.)

The long records from the Monterey station can be used to illustrate the temporal behavior of the forecast error and the influence of the wind-based corrections. The daily RMS current speed errors are plotted in Figure 33 with and without the wind-based corrections. Almost everywhere, the wind-treated forecasts, blue and black, are lower. Red and green tips are easily seen constantly at the top, despite the small difference.

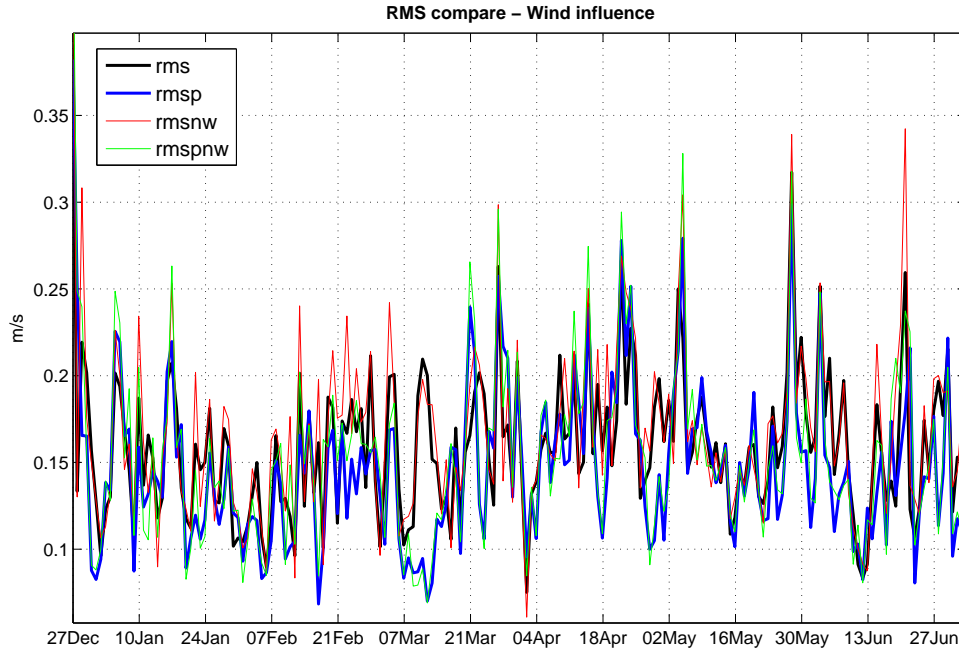


Figure 33. Zoom of a plot with the different calculated RMS – Wind influence. “p” is persistence, “nw” is no wind. (Monterey station.)

Zooming in on portions of the record (Figure 34) allows us to see the nature of some types of errors. As one example, sometimes, not often, the RMS associated with the tides treatment forecasts goes up with no apparent cause, probably the result of a bad frequency fitting.

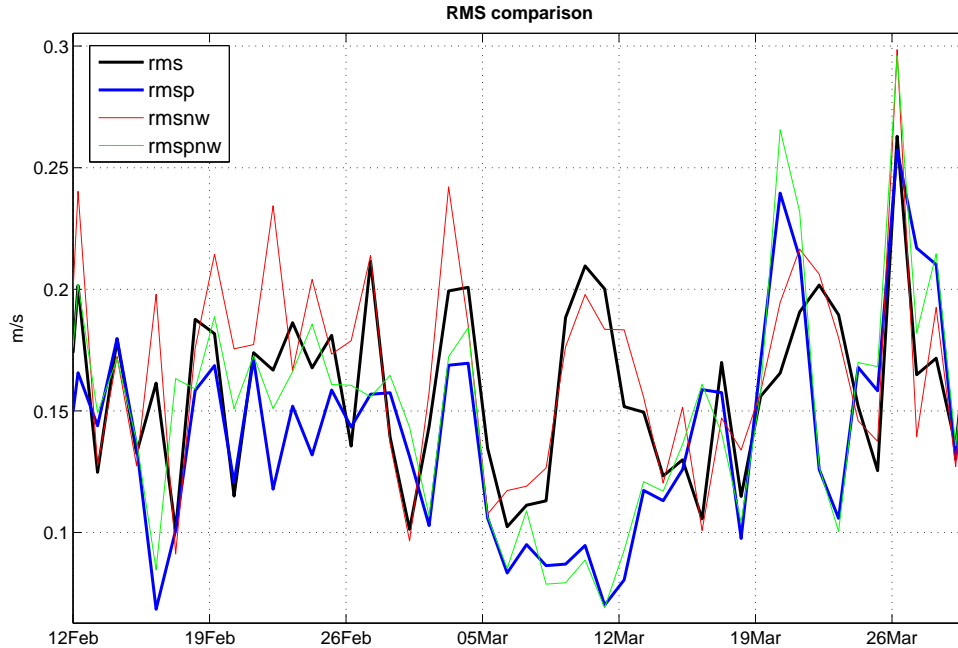


Figure 34. Zoom of a plot with the different calculated RMS – Possible tide problem. “p” is persistence, “nw” is no wind. (Monterey station.)

## F. ERROR CAUSES

If we take into account the average current velocities in this area, 0.17m/s, errors of 0.15m/s represent almost the same magnitude. Nevertheless, considering the main objectives of the application, having a measure of the uncertainty is a good result.

If we have a distress in a position where the rescue mean takes  $T$  time to fulfill the transit, with a  $C$  uncertainty current, after the transit the search area will be at least a circle of radius  $T \times C = M$  meters. Reducing the  $C$  will proportionally reduce  $M$ , which means that it will take less time to find the target.

The smaller the error, the bigger the odds of saving a life or reducing an oil spill’s impact. With this in mind, continuation of this research should be a priority of the naval sciences.

## 1. Accuracy Expectancy

In order for us to have an idea of what to expect in terms of accuracy, we need to layer known uncertainties related to the surface currents.

### *a. CODAR (From Wright, 2008)*

In a good scenario, we will have approximately 0.08m/s accuracy.

### *b. Winds*

The influence is unknown, but considered to be small, according to our transfer function result. The reading error multiplied by one order of magnitude below the induced current error.

### *c. Tides (Pawlowicz et al., 2002)*

Using the error output of  $t_{tide}$  and averaging the errors of the constituents, for one month, we have an uncertainty of around 0.020m/s. If we use 3 days the uncertainty is almost the same, 0.022m/s.

### *d. Growing Surface Waves (Ardhuin et al., 2003)*

This phenomenon may “induce stresses opposed to the wind stress for wave growth stages that may represent up to 10% of the wind stress for short fetches.” For a typical current, and according our transfer function, this represents an uncertainty of about 0.02m/s.

### *e. Eddy Surface Velocity*

In this study, a typical eddy speed variation over 24h is considered to be at least 0.02m/s. Eddies are highly variable but usually typical of certain locations. This uncertainty depends on the physical characteristics and if the eddy is influencing movement near the core or the out skirts. Observing the relative path is also important.

### *f. Others*

Other kinds of possible interferences were considered, but not included:

(1) Stokes Drift. For gravity waves:

$$U_s = a^2 \omega k \quad (15)$$

where  $a$  is the amplitude,  $\omega$  the frequency and  $k$  the wave number (Radko, 2007, Ocean Dynamics class notes NPS).

This yields for a 1m amplitude, 10s period, 10m length wave an induced velocity of 0.39 m/s, which means an order of magnitude similar to the total RMS error. Studies show that it may be opposed and cancelled by a Eulerian flow (Xu and Bowen, 1993; Monismith et al., 2006). Works are still in progress to evaluate the total waves i-duced flow.

(2) Inertial Movements. These play a role but depend on the local flow characteristics. They do not seem to play a major influence in the Monterey buoy area circulation. Its surface currents may be over 0.1 m/s, again the order of our RMS error. We have to take into account that if using yesterday's current for tomorrow, this error will be minimized. If we use tide treatment in a zone of important inertial motions, care should be taken before averaging for the mean flow.

(3) Other Non Linearities. (Eddies, larger periodicity waves, etc.) All of these influences exist and are a part of the flow. The use of persistency already takes into account enough of its magnitude.

The total sum of the uncertainties is 0.14m/s. Once these values were quantified in a conservative way, this means that the predictable accuracy is not expected to be better than the order of our actual results.

## **2. Abrupt Changes**

The plotting of RMS error against significant wave height (SWH) and current modulus (following Garfield et al., 2007) is almost intuitive and, by visual inspection, points out possible error causes. Wave, wind and current variations are shown as time series in Figure 35, together with the RMS forecast current error time series. Whenever an abrupt change exists in the current speed, RMS seems to go up. The wind acts against

this rise, decreasing the RMS each time it couples the change in the current. Wave height seems not to have a significant consistent impact. This impression is clearly supported in the zoomed time series presented in Figure 36.

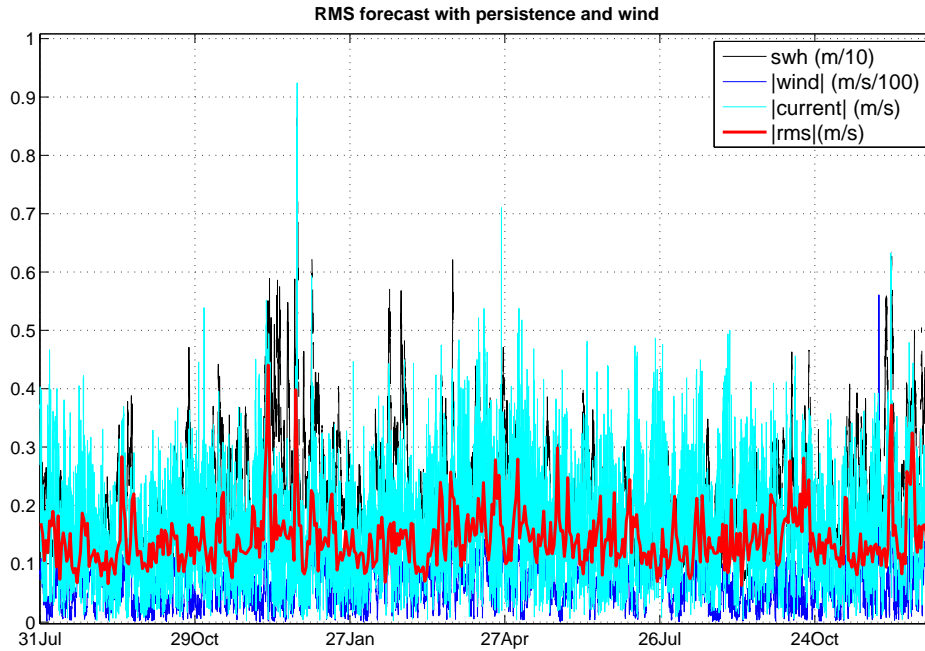


Figure 35. Full RMS plot versus SWH, current and wind. (Monterey station, Jul 06 to Dec 07.)

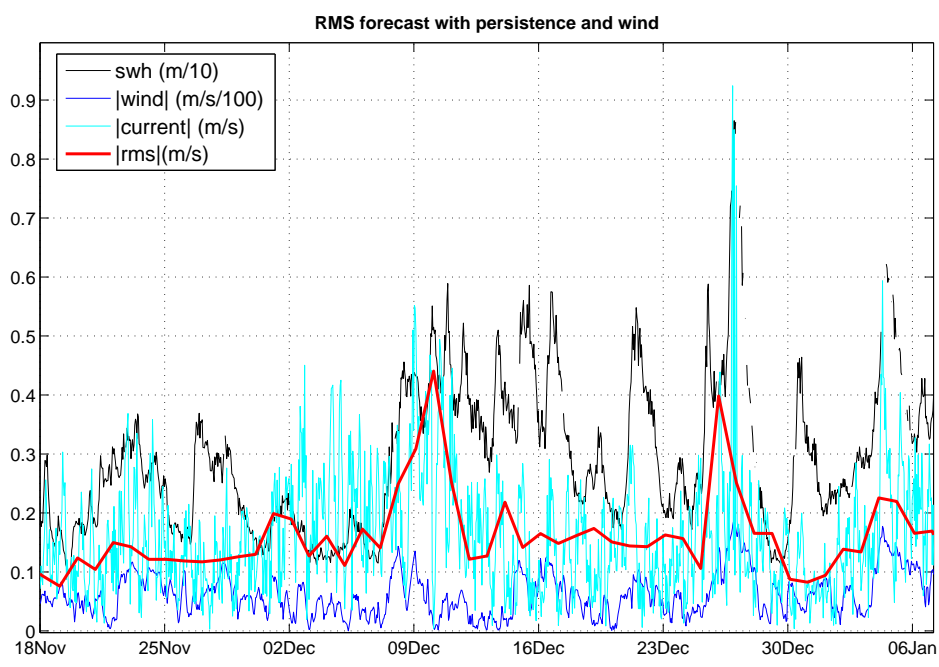
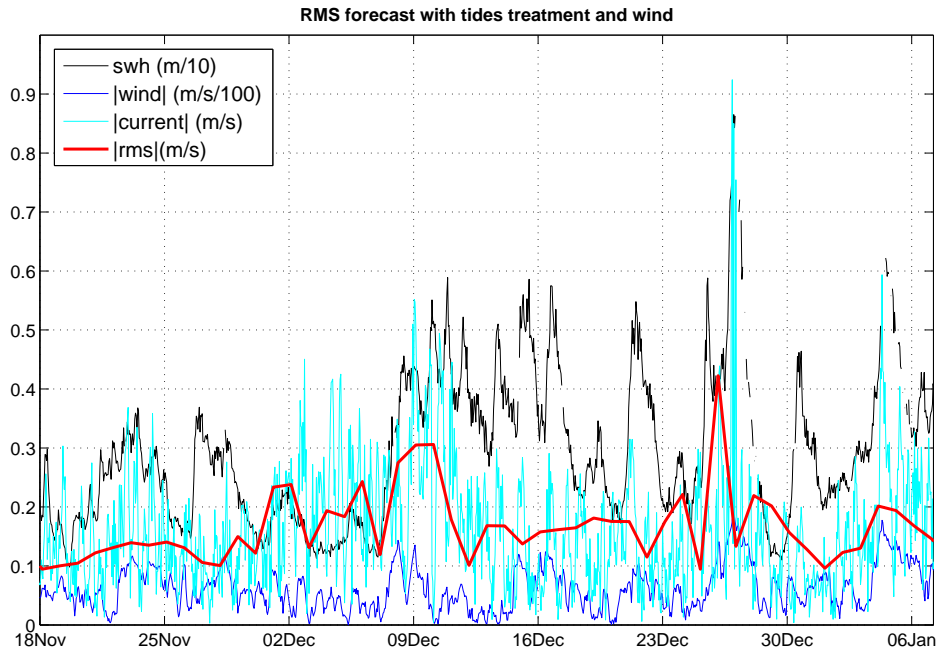


Figure 36. Zoom of RMS versus SWH, current and wind – High error seems associated with large current variation. Top with tides treatment. Bottom with persistence. (Monterey station.)

THIS PAGE INTENTIONALLY LEFT BLANK

## IV. CONCLUSIONS

This study analyzed long records of HF radar-derived surface currents and mooring-based wind observations for the region offshore Monterey Bay, California. The growth of HF radar instrumentation and the resulting surface current mapping data has enabled a number of scientific and public safety capabilities. In many instances, particularly with respect to search and rescue or spill mitigation applications, surface current *forecasts* are critical in addition to real time observations. To make accurate forecasts requires knowledge of background flow patterns plus variable flow patterns related to tides and wind-driven currents. The focus here has been on creating and testing models for wind-driven surface currents that are specific to the near-surface (~0.5m) depths of the HF radar observations.

The Monterey Bay region contains a wealth of surface observations from both HF radar and meteorological buoys. One site, in particular, surrounding the NOAA/NDBC buoy 46042 location has provided an eighteen-month, continuous set of currents and winds. Those data were used to develop an empirical transfer function between wind and HF radar-derived current. Shorter data sets from other buoy sites both inside and outside Monterey Bay were used to confirm results from the buoy 46042 location. In addition to the forward problem of creating a best-fit transfer function from wind to current, the recommended parameters were adjusted slightly by determining which values provided the most accurate 24-hour forecast of HF radar-derived surface current at the buoy 46042 location. The results of these wind versus surface current analyses from the 1.5 year dataset from five different stations lead to the following conclusions and requirements.

### A. THE WIND INFLUENCE

The wind induced current is on the order of 2% of the total wind speed, which is consistent with historical values. Despite this magnitude, the influence of introducing an explicit wind-driven current correction to the existing mean plus tidal current forecast models leads to around 10% of increased accuracy in the forecasts. The best results are obtained with a 50° clockwise rotation, and with a magnitude  $C_{wind} = 0.018U_5 + 0.018$ .

Although this study has shown a clear benefit to including a wind-driven correction, this correction is still below the level of the forecast uncertainties that derives from other uncorrected factors.

## **B. RESULT CAPABILITIES**

The overall result, including the wind-driven current correction, shows that HF radar-derived surface current mapping data are able to forecast surface currents in the next 24h with errors of about 0.15 +/- 0.1 m/s with 95% confidence. When significant changes in current happen without the wind influence, approximately one day of high RMS forecast error is expected. The largest and most persistent error events for the test period from July 06 to December 07 led to a four-day RMS error over 0.2 m/s.

## **C. NEXT STEPS**

The goal here has been to develop improvements to the short-term surface current forecast model, with primary focus on included the effects of predicted wind changes. Several other factors that are expected to influence the accuracy of 24-hour surface current forecasts were pointed out in Chapter III. The results here show that it will be necessary to understand and incorporate more of those influences if improvements beyond the 10% level achieved here are desired. The qualitative assessment of error sources presented in the last chapter, combined with previous work on HF radar surface current validation, suggests that errors in the measurements themselves may still be the biggest limitation to improved forecasts.

In addition to work that is ongoing to improve HF radar surface currents and error tracking, this study points to the need to begin to incorporate the most important aspect of HF radar observations into the forecast process. That is, *spatial* information from the surface current mapping data should be incorporated. At this time, all information about the sub tidal, tidal, and wind-driven surface currents that goes into the forecast models derives from time series information from a single location. HF radar, on the other hand, provides a map of surface currents every hour. Observations show those maps contain a good deal of horizontal variation in the surface currents, which is the fundamental reason that a network of HF radar systems is necessary for the transport applications supported

here compared with, for example, a single, moored current meter. The next generation forecast models should account for advective effects. The use of spatial integration between one calculated point and its immediate neighbors may allow gross errors to emerge more clearly.

THIS PAGE INTENTIONALLY LEFT BLANK

## LIST OF REFERENCES

- Ardhuin, F., B. Chapron, T. Elfouhaily, 2003: Waves and the Air-sea Momentum Budget: Implications for Ocean Circulation Modeling. *Journal of Physical Oceanography* (2004), **34**, 1741-1755.
- Ardhuin, F., L. Marié, N. Rasclé, P. Forget, A. Roland, 2008: Observation and estimation of Lagrangian, Stokes and Eulerian currents induced by wind and waves at the sea surface. French Service Hydrographique et Océanographique de la Marine, Ifremer, Université du Sud Toulon-Var and German Technische Universität Darmstadt. (Not yet published. Manuscript in final form).
- CODAR Ocean Sensors, 2008: References, bibliography and station picture. <http://www.codaros.com> (accessed September 2008).
- Ekman, V., 1905: On the influence of the Earth's rotation on ocean-currents. *Arkiv for Matematik, Astronomi och Fysik*, **2 (11)**, 1-52.
- Emery, W., D. Matthews, D. Baldwin, 2005: Mapping Surface Coastal Currents with Satellite Imagery and Altimetry. *Environmental research, engineering and management*, **2(32)**, 25-29.
- Foster, M., 1993: Evolution of Diurnal Surface Winds and Surface Currents for Monterey Bay. Master Thesis, Naval Postgraduate School.
- Garfield, N., J. Paduan, C. Ohlmann, 2007: Delivery and Quality Assurance of Short-Term Trajectory Forecasts from HF Radar Observations. Progress report submitted to the Coastal Response Research Center.
- Gonella, J., 1972: A rotary-component method for analyzing meteorological and oceanographic vector time series. *Deep-Sea Research*, **19**, 833-846.
- Kundu, P., 1975: Notes and Correspondence – Ekman Veering Observed near the Ocean Bottom. *Journal of Physical Oceanography*, **6**, 238-242.
- Martin, S., 2004: *An Introduction to Ocean Remote Sensing*. Cambridge, 266pp.
- McNally, G., D. Luther, W. White, 1988: Subinertial Frequency Response of Wind-Driven Currents in the Mixed Layer Measured by Drifting Buoys in the Midlatitude North Pacific. *Journal of Physical Oceanography*, **19**, 290-300.
- Monismith, S., E. Cowen, H. Nepf, J. Magnaudet, L. Thais, 2006: Laboratory observations of mean flows under surface gravity waves. *Journal of Fluid Mechanics* (2007), **573**, 131-147.

- Monterey Bay Aquarium Research Institute, 2008: Data and buoy pictures.  
<http://www.mbari.org> (accessed from March to September 2008).
- Mooers, C., 1973: Instruments and Methods – A technique for the cross spectrum analysis of pairs of complex-valued time series, with emphasis on properties of polarized components and rotational invariants. *Deep-Sea Research*, **20**, 1129-1141.
- National Oceanic and Atmospheric Administration, 2008: Data and buoy pictures.  
<http://ndbc.noaa.gov> (accessed from March to September 2008).
- O'Donnell, J., D. Ullman, M. Spaulding, E. Howlett, T. Fake, P. Hall, T. Isaji, C. Edwards, E. Anderson, T. McClay, J. Kohut, A. Allen, S. Lester, C. Turner, M. Lewandowski, 2005: Integration of Coastal Ocean Dynamics Application Radar (CODAR) and Short-Term Predictive System (STPS) Surface Current Estimates into the Search and Rescue Optimal Planning System (SAROPS). Report for the U.S. Department of Homeland Security, United States Coast Guard.
- Paduan, J., H. Graber, 1997: Introduction to High-Frequency radar: Reality and myth. *Oceanography*, **10**, 36-39.
- Pawlowicz, R., B. Beardsley, S. Lentz, 2002: Classical tidal harmonic analysis including error estimates in MATLAB using T\_TIDE. *Computers & Geosciences*, **28**, 929-937.
- Puleo, Jack, G. Farquharson, S. Frasier, K. Holland, 2002: Comparison of optical and radar measurements of surf and swash zone velocity fields. *Journal of Geophysical Research (2003)*, **108**, 45.1-45.12.
- Radko, T., 2007: Ocean Dynamics Class notes, Naval Postgraduate School.
- Ulman, D., J. O'Donnell, C. Edwards, T. Fake, D. Morschauser, M. Sprague, A. Allen, B. Krenzien, 2003: Use of Coastal Ocean Dynamics Application Radar (CODAR) Technology in U. S. Coast Guard Search and Rescue Planning. Report for the U.S. Department of Homeland Security, United States Coast Guard.
- Xu, Z., A. Bowmen, 1993: Wave and Wind-Driven Flow in Water of Finite Depth. *Journal of Physical Oceanography*, **24**, 1850-1866.
- Yelland, M., P. Taylor, 1995: Wind Stress Measurements from the Open Ocean. *Journal of Physical Oceanography (1996)*, **26**, 541-558.
- Wright, G., 2008: Validation of High Frequency Radar used in Ocean Surface Current Mapping via In-situ Drifting Buoys. Master Thesis, Naval Postgraduate School.

## BIBLIOGRAPHY

- Butman, B., M. Noble, D. Folger, 1979: Long-Term Observations of Bottom Current and Bottom Sediment Movement on the Mid-Atlantic Shelf. *Journal of Geophysical Research*, **84**, 1187-1205.
- Emery, W., R. Thomson, 1997: Data Analysis Methods in Physical Oceanography. Elsevier.
- Garfield, N., J. Paduan, C. Ohlmann, 2008: Delivery and Quality Assurance of Short-Term Trajectory Forecasts from HF Radar Observations. Progress report submitted to the Coastal Response Research Center.
- Herterich, K., K. Hasselmann, 1982: The horizontal Diffusion of Tracers by Surface Waves. *Journal of Physical Oceanography*, **12**, 704-711.
- Noble, M., R. Beardsley, J. Gardner, R. Smith, 1987: Observations of Subtidal Currents Over the Northern California Continental Slope and Adjacent Basin: Some Evidence for Local Wind Forcing. *Journal of Geophysical Research*, **92**, 1709-1720.
- Noble, M., B. Butman, 1979: Low-Frequency Wind-Induced sea Level Oscillations Along the East Coast of North America. *Journal of Geophysical Research*, **84**, 3227-3236.
- Noble, M., B. Butman, 1985: Wind-Current Coupling on the Southern Flank of Georges Bank: Variation with Season and Frequency. *Journal of Physical Oceanography*, **15**, 604-620.
- Paduan, J., K. Kim, M. Cook, F. Chavez, 2006: Calibration and Validation of Direction-Finding High-Frequency Radar Ocean Surface Current Observations. *IEEE Journal of Oceanic Engineering*, **31**, **4**, 862-875.
- Paduan, J., L. Rosenfeld, 2006: Remotely sensed surface currents in Monterey Bay from shore-based HF radar (CODAR). *Journal of Geophysical Research*, **101**, **C9**, 20,669-20,686.
- Weber, J., A. Melsom, 1992: Transient Ocean Currents Induced by Wind and Growing Waves. *Journal of Physical Oceanography*, **23**, 193-206.
- Zhang, Z., Y. Lu, H. Hsu, 2007: Detecting Ocean Currents from Satellite Altimetry, Satellite Gravity and Ocean Data. Dynamic Planet – International Association of Geodesy Symposia series, **130**, 17-22 (Chpt. 3), Springer Berlin Heidelberg.

THIS PAGE INTENTIONALLY LEFT BLANK

## INITIAL DISTRIBUTION LIST

1. Defense Technical Information Center  
Ft. Belvoir, Virginia
2. Dudley Knox Library  
Naval Postgraduate School  
Monterey, California
3. Dr. Jeffrey D. Paduan  
Department of Oceanography, OC/PD  
Naval Postgraduate School  
Monterey, California
4. Dr. Curtis A. Collins  
Department of Oceanography, OC/CO  
Naval Postgraduate School  
Monterey, California
5. Dr. Newell Garfield, Director  
Romberg Tiburon Center  
San Francisco State University  
Tiburon, California
6. Dr. Carter Ohlmann  
University of California  
Santa Barbara, California
7. LCDR Mesquita Onofre  
Portuguese Navy, Instituto Hidrográfico  
Lisbon, Portugal
8. CDR Cruz Martins  
Portuguese Navy, Direcção do Serviço de Formação  
Lisbon, Portugal
9. LCDR Calisto de Almeida  
Portuguese Navy, Instituto Hidrográfico  
Lisbon, Portugal